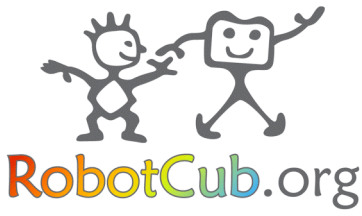

ROBotic Open-architecture Technology for
Cognition, Understanding and Behavior

Project no. 004370

RobotCub

Development of a cognitive humanoid cub

Instrument: Integrated Project
Thematic Priority: IST – Cognitive Systems

D 5.8 Synchronization and mirroring in imitative interaction games

Due Date: **01/09/2008**
Submission date: **05/09/2008**

Start date of project: **01/09/2004** Duration: **60 months**

Organisation name of lead contractor for this deliverable: **University of Hertfordshire**

Responsible Person: **Kerstin Dautenhahn**

Revision: **rev.no.**

Project co-funded by the European Commission within the Sixth Framework Programme (2002-2006)		
Dissemination Level		
PU	Public	PU
PP	Restricted to other programme participants (including the Commission Service)	
RE	Restricted to a group specified by the consortium (including the Commission Service)	
CO	Confidential, only for members of the consortium (including the Commission Service)	

Table of Contents

1 Executive Summary

This deliverable reports on studies carried out within RobotCub during the fourth project year concerning imitation scenarios involving interaction kinesics and attention. This work contributes to our understanding of the synchronization and mirroring interaction aspects in human-humanoid teaching and collaborative scenarios. Specifically, the work covers (a) the development of a new method for identifying similarity and synchronous behaviour in human-humanoid imitative interaction, (b) dynamical system modulation for robot skill acquisition from kinesthetic demonstrations, and (c) the relationship between the quality of imitation and attention behaviour in experiments where subjects imitate simple arm movements. The method in (a) is directly relevant for autonomously detecting synchronization and mirroring, the method in (b) for the matching of kinesics in humanoid imitation of humans, and (c) for the understanding of the role of kinesics in human-human imitation and lessons for ontogenetic humanoid robotics.

2 A Method for Identifying Similarity and Synchronous Behaviour between a Human and a Robot

At UNIHER a new method has been developed for identifying similarity and synchronous behaviour between a human and a robot interacting with each other, based on information theoretical methods developed by UNIHER in WP3 and WP6. We report on studies carried out which enable robots to identify similarity and synchrony between their actions and human actions. We consider this work to be stepping stone towards enabling a robot to learn socially from interaction with people. Being able to identify similarity and synchronicity (including when both human and robot actions are similar and perfectly asynchronous i.e. mirrored but perfectly out-of-phase) is important in allowing the robot to recognize human actions which are matching its own. It has been suggested that the identification of 'like me' in interaction may not only represent a salient event in the social development of an infant (cf. Meltzoff and Moore 1992), but, from the perspective of social robots (Dautenhahn 1994,1995), may enable a robot to engage in 'meaningful' interactions with its social environment as a key ingredient of learning in a social context.

A method for identifying these similar and synchronous actions is described here. While the method is not directly based on neurobiological modeling, we nevertheless employ a technique using computational principles that have been shown to model the perception-action loop of an agent acting in its environment in the language of information theory (Klyubin et al. 2004). Thus, the approach is deeply biologically inspired, but not on the level of neurons but on the more abstract level of information. The method employs the idea of similarity using *information distance*, previously described by Crutchfield (1990) and based on *information theory* (Shannon 1948). Information distance metrics have also been used in RobotCub work at UNIHER on sensorimotor map learning (WP3, e.g. D3.2, Olsson et al. 2006) and interaction history architecture for ontogeny based on grounded experiences (WP6, e.g. D6.4). Information distance is used here to capture the spatial and temporal relationships between behavioural events of interacting agents. Here the method is applied to a new context: namely, to particularly identify similarity and synchronicity instead of using it as a general correlation between sensor data. The experimental results suggest that this

method can indeed be employed successfully to identify similar and synchronous actions in human and robot imitation behaviour. Distinguishing informational matching in the interaction of an autonomous humanoid with a human via such methods is expected to help leverage social learning and communicative interaction in humanoid-human interactions in a manner to similar to the well-known naturally occurring mirroring and synchronization cues prevalent in non-verbal and verbal human-human interactions, including imitative interactions.

This work thus introduces a similarity identification method using an Information Distance methodology. We demonstrate that this method can successfully identify the similarity and synchronicity of behaviour between a human and a robot. We suggest that the application of appropriate binning strategies is the key factor that drives the effectiveness of this method. Experiments are carried out that initially validate the method on simulated data and then subsequently use real-world imitation game data. The results indicate that the method is able to correctly identify both perfectly synchronous and perfectly asynchronous imitating actions, distinguishing these from behaviour that is not mirrored or synchronized. Details of this work are presented in Appendix A (Shen et al 2008).

3 Imitation, Attention and Robot Learning via Kinesthetic Demonstrations

Work conducted at EPFL as part of WP5 is summarized in the papers attached in Appendices B and C (Hersch et al 2008, Just et al 2008). The latter is joint work with UNIFE. The first study is directly relevant for the matching of kinesics in humanoid imitation of humans and the latter to the understanding of the role of kinesics in human imitation.

In (Hersch et al 08), we further applied the Gaussian Mixture Modeling approach to learning tasks in acceleration space and compared to previous work of ours applying the same approach to learning tasks in velocity space. Results show that modeling in acceleration space allows to have a much more flexible model of the dynamics of the movements, and, most importantly, to be able to learn different dynamics depending on the location in space.

In (Just et al 2008), we investigate how control of simple point-to-point reaching movements could be modulated in imitation. In collaboration with the University of Ferrara, EPFL conducted a user-study in which subjects were asked to imitate in differed imitation reaching movements. We contrasted three conditions: transitive versus intransitive movements (directed or not at an object); left hand versus right hand motion; normal and abnormal movements. In the abnormal case, the demonstrator lifted the elbow exaggeratedly compared to normal. Subjects were unaware of the three conditions.

Kinematic data of the arm and direction of the imitator's gaze during the whole motion were recorded. Analysis of the data shows that there are mainly two categories of subjects: the "good" imitators and the "poor" imitators. In the first category ("good"

imitators), subjects reproduce accurately the kinematic features of the demonstrator's movements across all trials. In contrast the second category, ("poor" imitators), subjects reproduced the kinematic features of the movements only once their attention has been attracted to the arms of the experimenter by an unusual event (such swapping from using the right arm to using the left arm).

Fine analysis of the gaze direction across the different conditions show that there is a correlation between visual perception and reproduction of kinematic features of the movements. The accuracy of the reproduction is enhanced when the subject's attention is more spread out across the whole arm's motion.

References

[1] A. N. Meltzoff, M. K. Moore (1992), “Early imitation within a functional framework: The importance of person identity, movement and development,” *Infant Behavior and Development* 15:479-505.

[2] K. Dautenhahn (1994), “Trying to Imitate- a Step Towards Releasing Robots from Social Isolation,” in *Proceedings From Perception to Action Conference*, Lausanne, Switzerland, September 7-9, 1994, IEEE Computer Society Press, ISBN 0-8186-6482-7, edited by P. Gaussier and J-D. Nicoud, p 290-301

[3] K. Dautenhahn (1995), “Getting to know each other - artificial social intelligence for autonomous robots,” *Robotics and Autonomous Systems* 16, pp 333-356

[4] A. S. Klyubin, D. Polani, and C. L. Nehaniv, (2004). “Organization of the Information Flow in the Perception-Action Loop of Evolved Agents,” in *Proceedings of 2004 NASA/DoD Conference on Evolvable Hardware*, IEEE Computer Society.

[5] J. P. Crutchfield (1990), “Information and its Metric,” in *Nonlinear Structures in Physical Systems – Pattern Formation, Chaos and Waves*, Springer Verlag, 1990, pp 119-130.

[6] C. E. Shannon, “A mathematical theory of communication,” *Bell Systems Technical Journal,* vol. 27, pp. 379-423 and 623-656, 1948.

[7] L. Olsson, C. L. Nehaniv, D. Polani (2006), “From Unknown Sensors and Actuators to Actions Grounded in Sensorimotor Perceptions,” *Connection Science*, Vol. 18, Number 2, June 2006, pp. 121-144.

[8] A. Just, A. Billard, L. Craighero, A. D'Ausilio, A. Oliynyk and L. Fadiga, “Imitation and Focus of Attention” (in preparation). **[Appendix C]**

[9] M. Hersch, F. Guenter, S. Calinon and A. Billard, “Dynamical System Modulation for Robot Learning via Kinesthetic Demonstrations”, *IEEE Transactions on Robotics*, (2008). **[Appendix B]**

[10] Q. Shen, J. Saunders, H. Kose-Bagci, K. Dautenhahn (2008) Acting and Interacting like me? A method for identifying similarity and synchronous motor to interaction learning in robots" *Proceedings IEEE IROS workshop on "From motor to interaction learning in robots"* , September 26th 2008, Nice, France. **[Appendix A]**

Appendices

A. Q. Shen, J. Saunders, H. Kose-Bagci, K. Dautenhahn (2008) Acting and Interacting like me? A method for identifying similarity and synchronous behaviour between a human and robot. *Proceedings IEEE IROS workshop on "From motor to interaction learning in robots"* , September 26th 2008, Nice, France.

B. M. Hersch, F. Guenter, S. Calinon and A. Billard, Dynamical System Modulation for Robot Learning via Kinesthetic Demonstrations, *IEEE Transactions on Robotics*, (2008).

C. A.Just, A. Billard, L. Craighero, A. D'Ausilio, A. Oliynyk and L. Fadiga, Imitation and Focus of Attention (in preparation). DRAFT.

Acting and Interacting Like Me? A Method for Identifying Similarity and Synchronous Behavior between a Human and a Robot

Qiming Shen, Joe Saunders, Hatice Kose-Bagci, Kerstin Dautenhahn

Adaptive Systems Research Group, School of Computer Science
University of Hertfordshire, College Lane, Hatfield, AL10 9AB. United Kingdom

{Q.Shen, J.1.Saunders, H.Kose-Bagci, K.Dautenhahn}@herts.ac.uk

Abstract— This paper introduces a similarity identification method using an Information Distance methodology. We demonstrate that this method can successfully identify the similarity and synchronicity of behavior between a human and a robot. We suggest that the application of appropriate binning strategies is the key factor that drives the effectiveness of this method. Experiments are carried out that initially validate the method on simulated data and then subsequently use real-world imitation game data. The results indicate that the method is able to correctly identify both perfectly synchronous and perfectly asynchronous imitating actions.

1 Introduction

In order to exploit the opportunities that robots may offer in our daily lives, Human-Robot Interaction (HRI) has become an important topic [1]. A major research area in HRI is imitation behavior between humans and robots. A robot imitating a human may learn new skills, but also be able to engage more effectively in social interaction. Thus, a significant amount of effort has been devoted to this research topic (see, for example, [2, 3, 4, 5, 6, 7]) building on previous research in developmental psychology (such as facial imitation in infants and neonates [8]). Our current research focuses on preparatory works required to e.g. replicate human-infant experiments on the "like me" problem (see [9, 10, 11]).

In this paper we report on studies carried out which enable robots to identify similarity and synchrony between their actions and human actions. For example, a robot and human both waving their hands would indicate similarity of action, both waving in a mirror-like way would indicate synchronicity. We consider this work to be a stepping stone towards enabling a robot to learn socially from interaction with people. Being able to identify similarity and synchronicity (including when both human and robot actions are similar and perfectly asynchronous i.e. mirrored but perfectly out-of-phase) is important in allowing the robot to recognize human actions which are matching its own. It has been suggested that the identification of 'like me' in interaction may not only represent a salient event in the social development of an

infant (cf. [8]), but, from the perspective of social robots [9, 10], may enable a robot to engage in 'meaningful' interactions with its social environment as a key ingredient of learning in a social context. A method for identifying these similar and synchronous actions is described here[1]. While the method is not directly based on neurobiological modeling, we nevertheless employ a technique using computational principles that have been shown to model the perception-action loop of an agent acting in its environment in the language of information [12]. Thus, the approach is biologically inspired, but not on the level of neurons but on the more abstract level of information. The method employs the idea of similarity using *information distance*, previously described by Crutchfield [13] and based on *information theory* [14]. Information distance is used here to capture the spatial and temporal relationships between events. Relevant research using the information distance methodology as applied and further developed in developmental robotics in our research group has been described in, for example, [15, 16, 17]. In order to be consistent with this particular research approach, we utilize the same method but apply it to a different context, namely to particularly identify similarity and synchronicity instead of using it as a general correlation between sensor data. The experimental results suggest that this method can successfully identify similar and synchronous actions in human and robot imitation behavior.

This paper will explain the similarity identification method in section 2. In section 3 initial validation experiments using this method are described followed by actual experiments on a robot platform. In Section 4 the experimental results are analyzed and we discuss these results and future work in section 5.

2 Similarity Identification Using Information Distance

The similarity identification method introduced here calculates the information distance between human and robot body part trajectories to yield an indication of their similarity. The numeric size of the information distance value gives an indication of similarity, thus the more similar the behaviors, the lower the value. Similarly, a higher value for information distance indicates less similar behaviors.

The flow chart in Figure 1 shows the general approach of the similarity method. In this flow chart, circles and ellipses represent data components; rectangles with solid lines represent core processing components and rectangles with dashed lines represent optional processing components.

The general approach of this similarity method involves three stages: data collection, which consists of the first three components in the flow chart; pre-processing, which consists of the middle four components; and the information distance calculation, which consists of the last two components. These stages will now be described in more detail below.

[1] Note, our intention is not to propose a new method that outperforms others, but to demonstrate that a method based on information distance is suitable for the task of behaviour similarity detection, an approach that we are also using for other tasks in our computational robot control architectures.

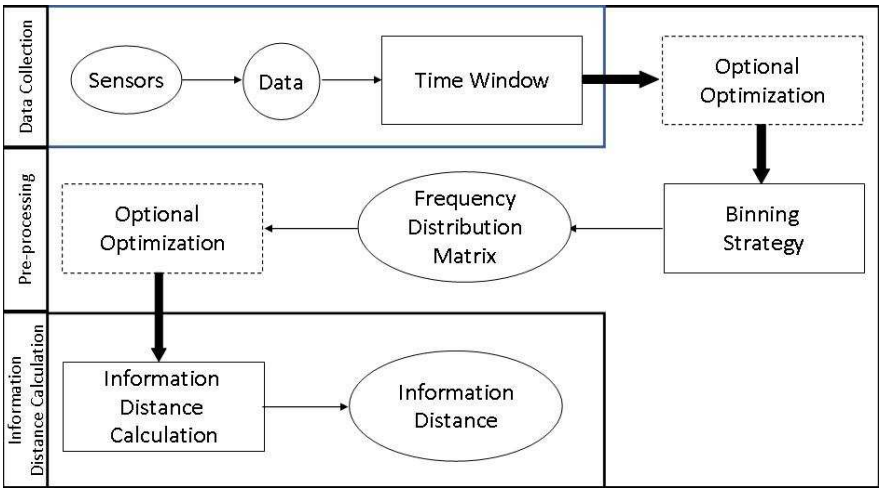

Fig. 1 The Similarity Method General Approach Flow Chart

2.1 Data Collection

In the data collection stage, a time window is used to store body parts' trajectory data of both the human and robot captured from sensors (including the internal states of the robot). For every time step, the time window is updated with the latest trajectory data collected.

The time window is a two dimensional array. One dimension is the number of time steps of the trajectory that the window can keep (treated as a row). The other dimension is the number of data items that are being tracked (treated as column). For example, if the spatial data currently being tracked is the 3-D co-ordinates of the hand position of both robot and human experimenter (x, y, z co-ordinates of the robot hand position and x, y, z co-ordinates of the human hand position) and the trajectory that is being kept is the most recent 50 time steps then a 50*6 array is allocated as the size of the time window. The size of the time window is fixed once allocated and uses a First-In- First-Out buffer to store new sensory data as it is recorded. Therefore, for each time step, the data at the back end of the window will be considered out of data and disposed of, with newly updated data added to the front end of the time window.

2.2 Binning Strategy

The data in the time window will be allocated into different bins according to its value and the binning strategy. Note that not all the data will be pre-processed at the same time. Every time the pre-process procedure is called, only two selected data columns are used. Similarly, every time the information distance calculation procedure is called, only two selected data columns are used. This is because the information distance can only be calculated between two items.

The binning strategy component is used to extract data distribution features. These features are recorded using a frequency distribution matrix and two bin frequency distribution arrays, which will be described below. They are the critical source of information to conduct the information distance calculation.

The bin frequency distribution matrix tracks how many times data items of bin x in column A appear together with data items of bin y in column B. The bin frequency distribution arrays track the number of times data items of each bin in their own column have appeared.

The two new binning strategies used in this similarity identification method, which we call *Partial-Adaptive Binning Strategy* and *Complete-Adaptive Binning Strategy* are both developed from the binning strategies described by Olsson [15], *Static Binning Strategy* and *Adaptive Binning Strategy*. However, they have significant differences due to the nature of the data in our research. In Olsson's work, the data represent pixel values of a robot's vision system, which have similar inputs. However, in the studies presented here, the input data are from different sources and may derive from different modalities. Therefore, there may be large variances in the data captured. Using the original binning strategies may cause a loss of a significant amount of information.

The newly developed binning strategies have three common factors: 'column-based independence', 'adaptive bin ranges' and 'tendency separation'. 'Column-based independence' means each column has an independent bin range. 'Adaptive bin range' means the bin range is determined by the maximum and minimum data entry within the same column. These two features cater for the fact that different columns contain data from different sensors and the range of their data values may have significant differences. Therefore, the features of different columns may be omitted if all the columns use the same bin range. 'Tendency separation' means the tendency of a data item (i.e. whether the next data item in the same column has a larger or smaller value than the current one) is considered in the bin allocation process. Practically, each bin is split into two bins: a rising bin and a descending bin. Once a data item is allocated into a bin, the tendency of this data item is examined. If the tendency is rising or staying still, the data is assigned to the rising bin. Otherwise, it will be assigned to the descending bin. Tendency separation is used to reduce the impact of the delay (or time-shift) between one agent imitating another's behavior. For example, there might be a slight delay between a human copying the actions of a robot, or vice-versa.

An example of time shift impact is presented in Figure 2. Curve A and curve B are identical except curve B is slightly shifted. Although point *a* and point *b* on curve B have the same value, the difference between their corresponding points (*c* and *d*) on curve A is significant. If only data value is considered, point *a* and point *b* will be allocated to the same bin. However, the bins that *a* and *b* belong to have the same chance of corresponding to the two bins that *c* and *d* belong to. Consequently, this one-to-many relationship causes an ambiguity and omits the fact that there is one-to-one relationship existing if the slope factor is considered. Figure 3 shows a robot and human forearm X-axis trajectory (where a human was attempting to replicate a robot movement) and illustrates the existence of this time shift impact in real life. During the imitation interaction, it is almost impossible to synchronize robot and human

behavior perfectly. There are always some differences in timing between the two behaviors.

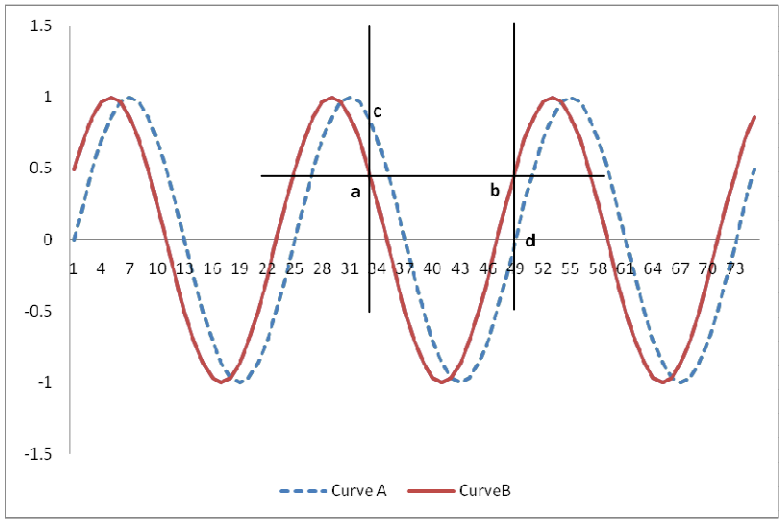

Fig. 2 Time Shift Impact Example

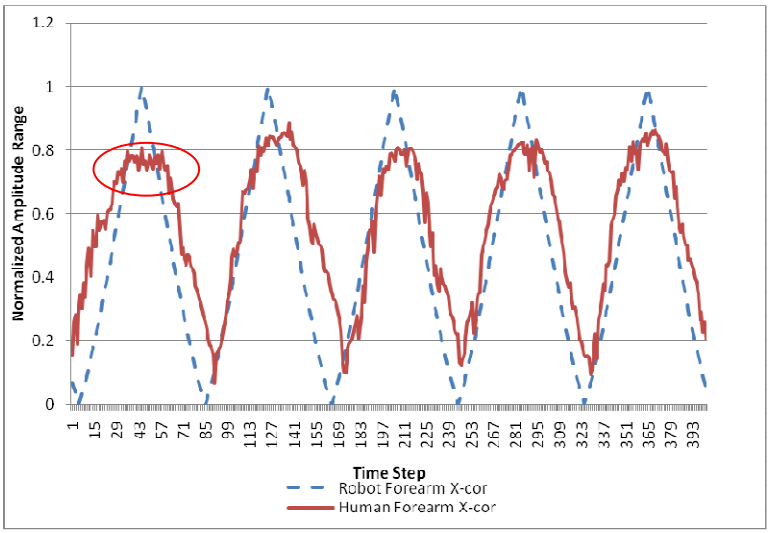

Fig. 3 Robot and Human Forearm X-axis Trajectory

The difference between the *partial*-adaptive binning strategy and the *complete-adaptive binning strategy* is whether the bin size can adapt to the incoming data. The *partial-adaptive binning strategy* has a fixed bin size which only varies as the

consequence of the variance of the bin range. The *complete-adaptive binning strategy* allows the bin size to vary in order to ensure that each bin has the same number of data items.

The application of different binning strategies may entirely change the output results from the information distance calculation. As a binning strategy is applied prior to the input of the information distance calculation, changes made to the binning strategy will cause changes to the data distribution features extracted. Hence, the choice of the binning strategy will have an impact on the final output of the entire approach.

2.3 Pre- and Post-binning optimization

This sub-section introduces the processing components of the pre-processing stage excluding the binning strategy component. There are two optional optimization components in this stage. The one prior to the binning strategy component is called *pre-binning-optimization* and the other is called *post-binning-optimization*.

The purpose of *pre-binning-optimization* is to reduce the impact of errors occurring during the data collection stage (such as sensor misdetection). The pre-binning-optimization component consists of two optional sub-components: *curve smoothing* and *normalization*.

Curve smoothing filters the "zig-zag" parts of the human forearm X-axis trajectory curve (illustrated in a ellipse in Figure 3). These "zig-zag" parts may arise from two factors: either the human imitation behavior is not performed smoothly, or the sensors are affected by environmental noise. This may confuse the binning strategy component in detecting the forearm movement tendency. The current strategy applied to curve smoothing is to take the average value of the original data point and its neighbors as the new data point. The effect of this curve smoothing approach is presented in Figure 4.

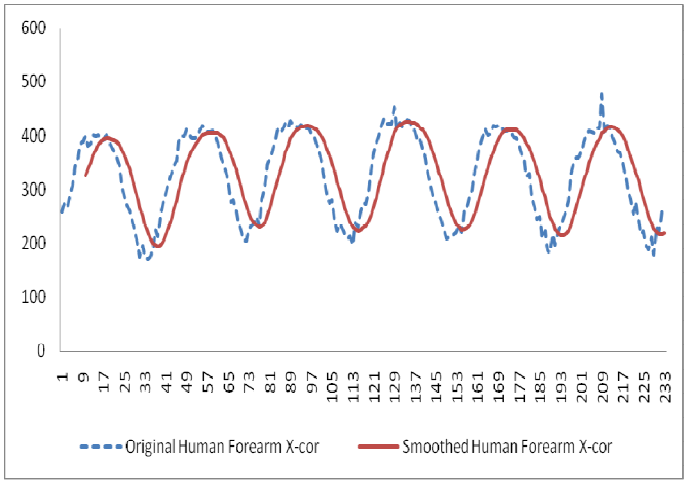

Fig. 4 The Effect of Curve Smoothing

Normalization reduces the impact of inconsistent amplitude, which can be observed in Figure 3. Whether it is appropriate to apply the normalization sub-component depends on the nature of incoming data. If the incoming data curve is supposed to have consistent amplitude, normalization may filter the error in amplitude. Otherwise, application of normalization may cause misleading results. The general strategy is:

1. set the nearest 'hill' to 1 and the nearest 'valley' to 0;
2. the normalized value of the data between hill and valley = (current data value – original valley data value) / (original hill data value – original valley data value)

The purpose of *post-binning-optimization* is to reduce the data distribution range and therefore enhance the one-to-one relationship between bins from the two data columns being compared. The stronger the one-to-one relationship between two bins is, the more likely they are to be correlated. The higher the correlation of the bins between two data columns, the more likely the two data columns are correlated. That is, in the context of this paper, these two data columns are "similar".

The current post-binning-optimization methodology we use is called "winner take neighbors". If bin *a* in column A appears with bin *b* in column B more often than any other bin in column B, then bin *b* will add the number of times its two neighbor bins in column B appear with bin *a* to its own number. Thus, the one-to-one relationship between bin *a* and bin *b* is enhanced.

2.4 Information Distance Calculation

The calculation of information distance between two data columns, usually a pair of corresponding behavior components from the human and robot behavior respectively (for example, the x co-ordinates of the human forearm position and the x co-ordinates of the robot forearm position), is based on the information metric described by Crutchfield [13]. The information distance between two data columns X and Y is defined as the sum of two conditional entropies of these two columns [15]. It can be calculated using the following formula [15]:

$$d(X,Y) = 2 * H(X,Y) - (H(X) + H(Y)) \qquad (1)$$

The entropies presented in the above formula can all be derived from the data distribution features extracted using binning strategies. The joint entropy of column X and Y can be calculated using the frequency distribution matrix and the entropy of X and Y can be calculated from frequency distribution arrays. For more details of the information distance calculation, please refer to [15] and [16].

3 Experimental Setup

The robot used in the following experiments is a minimally expressive humanoid robot called KASPAR, and was developed by the Adaptive Systems Research Group at the University of Hertfordshire. KASPAR is a child-sized humanoid robot with 14 degrees of freedom (8 in head and 6 in arms) [18]. The robot has been designed specifically for the purpose of engaging people in socially interactive behaviour. The robot is e.g. able to perform certain face, head and arm gestures that have been used in human-humanoid imitation games e.g. with children (see figure. 5 and [19]).

Fig. 5: KASPAR (The KASPAR figure is sourced from [18])

A marker-detection toolkit ARToolkit [20] is used in the experiments to detect human body parts. Other object detection approaches such as face detection, color object detection and gray-scale object detection have also been explored. However, the marker-detection approach using ARToolkit is relatively reliable and it can return an object's spatial data to track the position of the object.

As a starting point in the investigation of the method presented, the behavior to be imitated is not expected to be complex. Therefore, the behavior chosen involves only forearm waving while the upper arm is kept stationary. This reduces the complexity of the imitation. The correspondence problem [21] in the imitation behaviors is solved explicitly by mapping human elbow joint angles to robot elbow servo readings.

4 Experiment Results and Analysis

The first set of experiments was conducted to validate the similarity identification method. Please note that in the validation experiments, no optional optimization strategy is applied because all these three experiments are testing the most basic theoretical method.

4.1 Similarity Identification Method Validation Experiments

In order to validate whether this similarity identification model can at least process the data in the right way, a validation process was conducted.

4.1.1 Random Data Validation

The first step of validation is to use randomly generated data columns to check whether the similarity identification model using the partial-adaptive binning (SIM-PB) or complete-adaptive binning (SIM-CB) can identify identical data columns. The results show that both SIM-PB and SIM-CB can find identical data columns as the resulting information distance between them is 0.

4.1.2 Artificial Data Validation

The second step of validation is to use 3-D co-ordinates generated by Matlab [22] which models the waving behaviors between the human and the robot. Compared with the recorded data from the experiments, the modeled data is a much simpler. In this model, the waving behavior of the human and the robot are completely synchronized. There is very little difference between the 3-D position co-ordinates of the human and robot forearm caused by the different arm length settings. The results show that both SIM-PB and SIM-CB can identify very similar behaviors as the resulting information distance between them is 0.

4.1.3 Sine Curve Data Validation

The third step in the validation is to use sine curve data to check how SIM-PB and SIM-CB can handle time step shifts. That is, SIM-PB and SIM-CB will calculate the information distance between the original sine curve and the shifted sine curve. The time step shifts are used to simulate behavioral delay problems in real life. If SIM-PB and SIM-CB can successfully identify similar curves with a small number of time step shifts, it is very likely that they can also identify reasonably delayed imitation behaviors. A sine curve was chosen because it is an ideal continuous periodic data model and the repeated waving behavior is also continuous and periodic. In this validation step, the number of time steps shifted will continuously increase until one entire period is shifted. The performance of SIM-PB and SIM-CB is recorded during shifting. An example of shifted sine curve is presented in Figure 6.

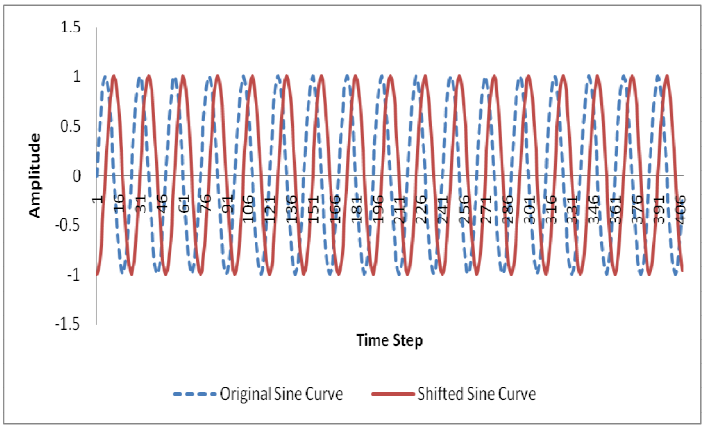

Fig. 6 Sample Sine Curve Used in Sine Curve Data Validation

A result of the validation of SIM-PB is shown in Figure 7. Please note that although there are some special cases due to the assignment of data entries with the same value into the same bin regardless of whether this bin has reached its capacity limit, in general the results outlined are similar to the curve in Figure 7.

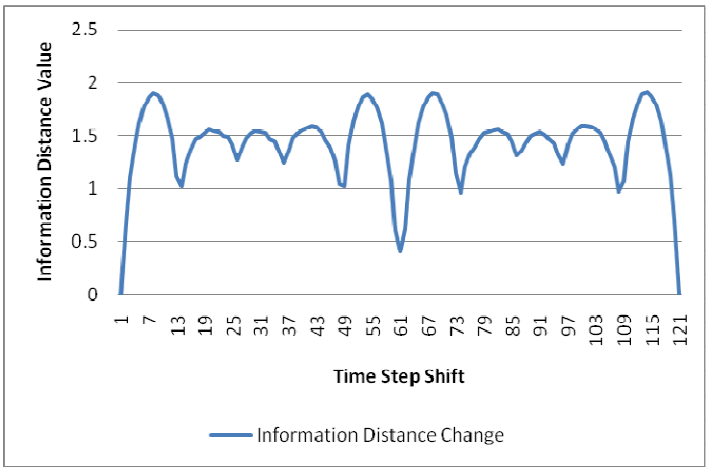

Fig. 7 Sine Curve Data Validation Result

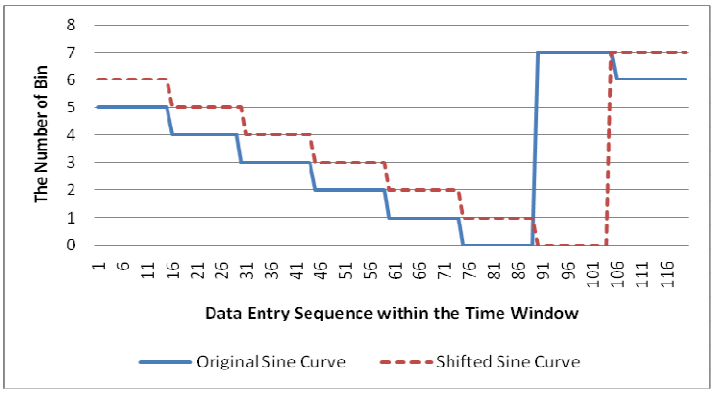

Fig. 8 Relationship between Bins at A Local Minimum

From this figure (which shows the SIM-CB results, SIM-PB gave similar results but is not shown) it is clear that there are three points during the entire process where the information distance between the two curves falls to a low value. As one entire period of the sine curve has 120 time steps, at the 1st time step and 121th time step, the two sine curves are actually on top of each other. That is why the information distance between them is 0. At the 61th time step, when the two sine curves are completely out of phase (become perfectly asynchronous), the information distance

between them also goes down. As both mappings (completely in phase and out of phase) indicate the existence of information correlation, the validation can be considered as successful. Thus the method serves to indicate both when the human is (mirror) matching the actions of the robot, and also when the human is matching but is perfectly out of phase, both of which may be considered to be synchronous behaviors. In addition, it also shows that the method is sensitive to the delay because once there is a small number of time step shifts, the information distance rises immediately (and effectively means that the human and the robot are not synchronized). The local minimums in the curve indicate the existence of strong one-to-one relationship. An example is shown in Figure 8. Bin 0, 1, 2, 3 are the descending bins in Figure 8 and bin 7, 6, 5, 4 are the corresponding rising bins.

4.2 Experiments Using Imitation Game Data

The above validation demonstrated that the performance of SIM-PB and SIM-CB met the requirements, i.e. they can successfully identify very similar or identical data columns. Therefore, this similarity identification model was then applied to real human-robot interaction data.

The data used for these experiments were the recordings of three imitation game scenarios. In the first scenario, the human experimenter imitated the forearm waving behavior of the robot (called synchronous imitation). In the second scenario, the human experimenter was imitating the forearm waving behavior of the robot, however, in a different direction (called out of phase imitation – or perfectly asynchronous behavior). In the third scenario, the human experimenter does not do anything when the robot is moving and waves when the robot is doing nothing (called unsynchronized behavior). The results achieved are shown in Figure 9.

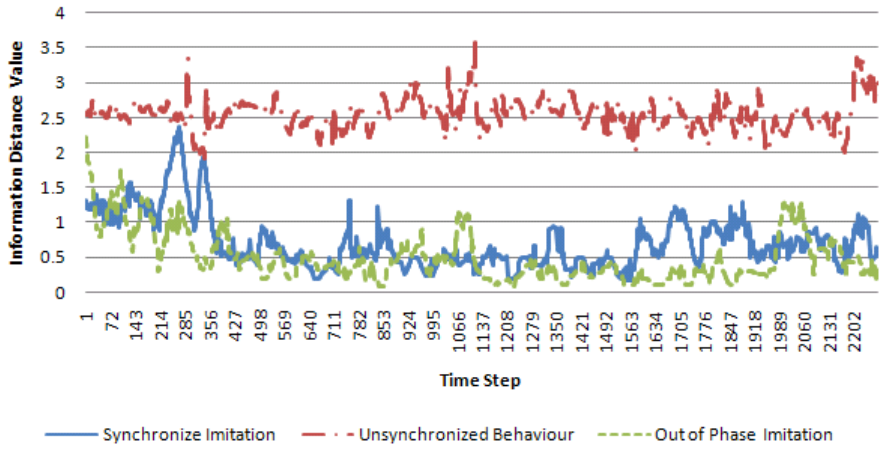

Fig. 9 Result of Experiments Using Imitation Game Data

The results shown in Figure 9 imply the similarity identification model can successfully identify the similarity between robot and human imitation behavior as both the synchronous and out-of-phase imitation curves are visibly separated from the unsynchronized behavior curve. There are two noticeable phenomena: 1) the unsynchronized behavior information distance curve is significantly higher than the synchronized imitation curve and the out-of-phase imitation curve; 2) the synchronized imitation curve is close to the out-of-phase imitation curve. The first phenomenon matches the result expected from information distance calculation: events having less similarity have higher information distance values and vice versa. The second phenomenon matches the results in Figure 7: when two curves are closer to synchronized or completely out of phase, the information distance between them is lower.

The positive results in the experiments also suggest the importance of the binning strategies. If improper binning strategies are used in this model then the results may be very different. The results presented in Figure 10 are derived from the same similarity identification model except for a change of the binning strategy component, in this case the strategy lacks the tendency separation feature. This weakens the one-to-one correspondence between bins and therefore leads to a different result with less clear separations between the curves.

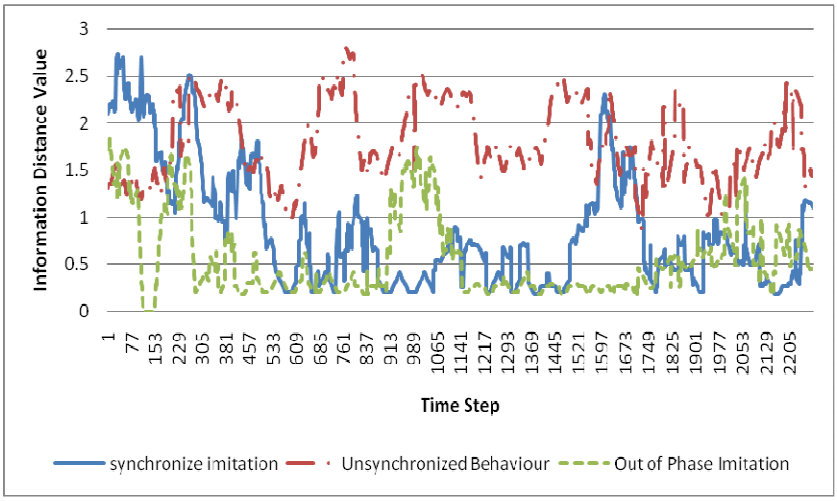

Fig. 10 Results of Using an Improper binning strategy

5 Discussion and Further Work

The experimental results illustrated in section 4 indicate that using the method is able to correctly identify similarity and synchronous behavior between a human and a robot. In real-world human robot imitation interaction, an information distance threshold can be set to explicitly identify the similar and synchronous behaviors.

Therefore, a robot can recognize that a human's action matches its own behavior if the current information distance is within the threshold limit. A mechanism of adapting the threshold is required because different experimental parameter settings and different binning strategies may change the range of information distance.

People may argue what the proper binning strategy is for a particular experiment. Based on this study, a proper binning strategy should retain the most important correlation among the experimental data. Understanding the nature of the experimental data can help to choose or design a proper binning strategy. A validation process then needs to be applied to evaluate the results.

Other approaches, such as Pearson's correlation coefficient calculation, can also identify similar behaviors. However, in this paper, we are not attempting to compare methods, rather we are suggesting this method to complement other approaches. Additionally, we also find that the application of appropriate binning strategies is the key factor that drives the effectiveness of this method. It is because the binning strategy in this information distance method acts as an information filter. An inappropriate binning strategy can cause undesired information loss. Another critical issue of the binning strategy application, which is not presented in this paper, is the choice of the number of bins, where it can be argued as to the number of bins needed, there being no ideal number for all tasks.

Building on the information distance method, further research will investigate how a robot can identify the existence and quality of imitation behaviors during human-robot interaction. Having achieved the above stage, e.g. imitation games that replicate human-infant experiments on the "like me" problem will be conducted to investigate how a robot can acquire and develop social behavior through imitation interaction with humans.

References

[1] J. A. Adams and M. Skubic (2005), "Introduction to the special issue on human–robot interaction," in *IEEE Trans. Syst., Man, Cybern. C, Appl. Rev.*, vol. 35, no. 4, pp. 433-437.

[2] A. Alissandrakis, C. L. Nehaniv, K. Dautenhahn (2006) "Action, State and Effect Metrics for Robot Imitation," in *Proc. The 15th IEEE International Symposium on Robot and Human Interactive Communication* (RO-MAN06), University of Hertfordshire, Hatfield, United Kingdom, 6-8 September, 2006, pp. 232-237

[3] A. Alissandrakis, C. L. Nehaniv, K. Dautenhahn, J. Saunders (2005) "Achieving corresponding effects on multiple robotic platforms: Imitating in context using different effect metrics," in *Proc. AISB'05 Third International Symposium on Imitation in Animals and Artifacts*, 12-14 April 2005, University of Hertfordshire, UK, pp. 10-19.

[4] M. Ito and J. Tani (2004), "Joint attention between a humanoid robot and users in imitation game," in *Proc. 3rd Int. Conf. on Development and Learning (ICDL'04)*, La Jolla, U.S.A., 2004.

[5] A. Billard and M. J. Matarić (2001), "Learning human arm movement by imitation: evaluation of a biologically inspired connectionist architecture," in *Robotics and Autonomous Systems* 941, pp 1-16.

[6] C. A. Acosta-Calderon and H. Hu (2004), "Robot imitation: A matter of body representation," in *Int. Symposium on Robotics and Automation ISRA 2004*, Queretaro, Mexico, 2004, pp 137-144.

[7] C. A. Acosta-Calderon and H. Hu (2005), "Robot imitation from human body movements," in *Proceedings of the 3rd Int. Symposium on Imitation in Animals and Artifacts, AISB'05 Convention*, University of Hertfordshire, Hatfield, England, 12-15 April 2005, pp1-9.

[8] A. N. Meltzoff, (1997). "Explaining Facial Imitation: A Theoretical Model," in *Early Development and Parenting*, Vol. 6, pp. 179-192.
[9] K. Dautenhahn (1994), "Trying to Imitate- a Step Towards Releasing Robots from Social Isolation," in *Proceedings From Perception to Action Conference*, Lausanne, Switzerland, September 7-9, 1994, IEEE Computer Society Press, ISBN 0-8186-6482-7, edited by P. Gaussier and J-D. Nicoud, p 290-301
[10] K. Dautenhahn (1995), "Getting to know each other - artificial social intelligence for autonomous robots," in *Robotics and Autonomous Systems* 16, pp 333-356
[11] J. Nadel, I. Carchon, C. Kervella, D. Marcelli, & D. Réserbat-Plantey, (1999). "Expectancies for social contingency in 2-month-olds." In *Developmental Science*, 2, 164-173.
[12] A. S. Klyubin, D. Polani, and C. L. Nehaniv, (2004). "Organization of the Information Flow in the Perception-Action Loop of Evolved Agents," in *Proceedings of 2004 NASA/DoD Conference on Evolvable Hardware*, IEEE Computer Society.
[13] J. P. Crutchfield (1990), "Information and its Metric," in *Nonlinear Structures in Physical Systems – Pattern Formation, Chaos and Waves*, Springer Verlag, 1990, pp 119-130.
[14] C. E. Shannon, "A mathematical theory of communication," *Bell Systems Technical Journal*, vol. 27, pp. 379-423 and 623-656, 1948.
[15] L. Olsson, C. L. Nehaniv, D. Polani (2006), "From Unknown Sensors and Actuators to Actions Grounded in Sensorimotor Perceptions," in *Connection Science*, Vol. 18, Number 2, June 2006, pp. 121-144.
[16] Lars Olsson, (2006), "Information Self-structuring for Developmental Robotics: Organization, Adaptation, and Integration," PhD thesis, University of Hertfordshire, 2006.
[17] N. A. Mirza, C. L. Nehaniv, K. Dautenhahn, and R. te Boekhorst, (2007) "Interaction histories: From Experience to Action and Back Again," in *Proceedings of the 5th IEEE International Conference on Development and Learning (ICDL 2006)*. ISBN 0-9786456-0-X.
[18] University of Hertfordshire (2007), "KASPAR, Kinesics And Synchronisation in Personal Assistant Robotics," http://kaspar.feis.herts.ac.uk, last accessed 24 October, 2007.
[19] B. Robins, K. Dautenhahn, R. te Boekhorst, C. L. Nehaniv (2008) "Behaviour Delay and Robot Expressiveness in Child-Robot Interactions: A User Study on Interaction Kinesics," In *Proc. ACM/IEEE 3rd International Conference on Human-Robot Interaction (HRI 2008)*.
[20] H. Kato, M. Billinghurst (1999) "Marker Tracking and HMD Calibration for a video-based Augmented Reality Conferencing System," in *Proceedings of the 2nd International Workshop on Augmented Reality (IWAR 99)*, San Francisco, USA. October, 1999.
[21] C. L. Nehaniv and K. Dautenhahn (2001). "The Correspondence Problem," in *Imitation in Animals and Artifacts*. MIT Press, 2002.
[22] The MathWorks, Inc. (2008), "MATLAB – The Language of Technical Computing," http://www.mathworks.com/products/ matlab/, last accessed 15 Feb, 2008

Dynamical System Modulation for Robot Learning via Kinesthetic Demonstrations

APPENDIX B

Micha Hersch, Florent Guenter, Sylvain Calinon, and Aude Billard
Learning Algorithms and Systems Laboratory - LASA
School of Engineering - EPFL
Station 9 - 1015 Lausanne - Switzerland

Abstract

We present a system for robust robot skill acquisition from kinesthetic demonstrations. This system allows a robot to learn a simple goal-directed gesture, and correctly reproduce it despite changes in the initial conditions, and perturbations in the environment. It combines a dynamical system control approach with tools of statistical learning theory and provides a solution to the inverse kinematics problem, when dealing with a redundant manipulator. The system is validated on two experiments involving a humanoid robot: putting an object into a box, and reaching for and grasping an object.

Index Terms

Robot Programming by Demonstration, Dynamical System Control, Gaussian Mixture Regression

Corresponding author: Micha Hersch, micha.hersch@epfl.ch
Conditionally accepted short paper submitted to the IEEE Transactions on Robotics
Paper # A07-471/A06-417

This work was supported by the European Commission through the EU Integrated Projects ROBOT-CUB (FP6-IST-004370), Cogniron (FP6-IST-FET-002020) and ROBOT@CWE (FP6-034002).

Dynamical System Modulation for Robot Learning via Kinesthetic Demonstrations

I. Introduction

As robots are progressively coming out of the controlled environment of assembly lines to pervade the much less predictable domestic environments, there is a need to develop new kinds of controllers that can cope with changing environments and that can be taught by unskilled human users. In order to address this last issue, *Programming by Demonstration* (PbD) has emerged as a promising approach [1]. This approach differs significantly from classical approaches to robot manipulation. Those approaches typically start by modeling the task, the relevant elements of the environment and the robot, as well as their dynamics. The problem is then to find the adequate robot command that will bring the whole system into a desired state specified by the programmer. This is usually done by using the plant model and sensor information to estimate the state of the world, and finding a control law specifying the command adequate to various states of the world. This law can be hard-coded, e.g. for juggling [2], grasping [3], 2D pushing and throwing [4], or obstacle avoidance for reaching [5]. But it can also be (partially) learned from (possibly simulated) exploration, e.g. for stable grasping [6] or object manipulation under wrench closure constraints [7]. In PbD, the idea is to try to extract an adequate control law from demonstrations of the task performed by a human. The demonstrations can indeed provide useful information, for example appropriate grasps in a grasping task [8] (see [1] for a further discussion of the use of PbD for robot control). PbD has been mostly used in two cases: for tasks involving no or very loose interaction with the environment (like writing, martial arts or communicative gestures) human demonstrations are used to train a movement model, which can be used to reproduce the task. Those movement models (also used in computer animation or visual gesture recognition) usually imply some averaging process (LWR [9], HSTMM [10]), possibly in a latent space (GPLVM [11], ST-Isomap [12]) or some probabilistic model like HMMs [13] or Bayesian Networks [14]. And for more complex tasks, involving precise interactions with the environment, the robot learns from examples how to sequence a set of hard-coded controllers for a given task. This has been done using HMMs [15] or knowledge-based systems [16].

In our work, we position ourselves in between those two approaches. The tasks we consider (such as reach-to-grasp) require some interaction with the environment, while remaining relatively simple. Like the first approach, we train a motion model for the task, and like the second approach, we also use a hard-coded controller. We start with a basic built-in controller consisting in a dynamical system with a single stable attractor. We then learn a task model used to modulate the trajectories generated by the dynamical system in a way appropriate for a given task. This results in a general framework for learning and reproducing goal-directed gestures, despite different initial conditions and changes occurring during task execution. In this respect it is an improvement on [17], which also learns reach-to-grasp movements, but in a static setting.

The closest work to ours is [9], which uses a dynamical system for goal-directed reaching. There, a desired trajectory in joint space is obtained from a single demonstration and is embedded in a dynamical system, which can reproduce the qualitative features of this trajectory, while reaching a somewhat different target from a different initial position. In a previously published paper [18], we learned a velocity profile from demonstrations and used it to modulate a dynamical system acting on the end-effector. The novelty of the present contribution with respect to those last two papers is the following. First, while [9] learns a trajectory in joint space, and [18] is controlling in task space, here we propose a hybrid task and joint space controller, which can combine the advantages of both. The second and more fundamental difference lies in the level of generalization. Whereas [9] tries to reproduce a *single joint angle trajectory*, and [18] learns a *task specific velocity profile*, here we learn a whole *dynamical system* capturing the *correlations across multiple variables* for a given task. This enables us to present results that are not mere trajectory comparison (as in [9]), but that quantify the adaptivity of our controller at the level of task success rate. We show experimentally that modeling the task as a dynamical system yields a more adaptive controller.

In those experiments, the motions are demonstrated to the robot by a human user moving the robots' limbs passively (kinesthetic training). We consider two tasks, placing an object into a box, and reaching-to-grasp a chess piece, see Fig. 2 for illustrations of these two tasks.

II. Overview

The system is designed to enable a robot to learn to modulate its generic controller to produce arbitrary goal-directed motion. The model must be generic so as to reproduce the motion given different initial conditions and under perturbations during execution. Moreover, the architecture of the system must permit the use of different control variables for encoding the motion. Here, we compare a motion encoding either as a velocity profile or as an acceleration field. We refer to those further as the *velocity model* (see Section II-B) and the *acceleration model* (see Section II-C).

A. System Architecture

The structure of the system is the same for both models and is schematized in Fig. 1. During training, the relevant

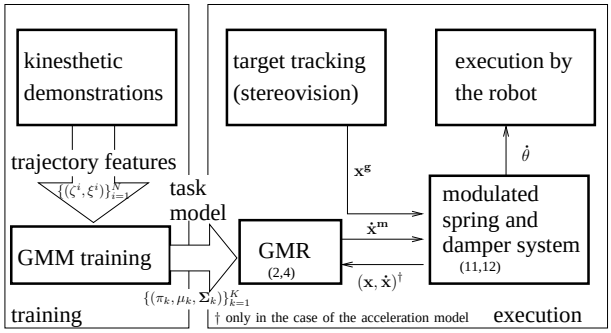

Fig. 1. The architecture of the system. During training the relevant variables (end-effector's position, velocity and acceleration) are extracted from the demonstrations and used to train a GMM. During task execution, this model is used to modulate a spring-and-damper system. $\dot{\mathbf{x}}^{\mathbf{m}}$ is the end-effector velocity specified by the task model. $\mathbf{x^g}$ is the target location, and $\mathbf{x}^*, \dot{\mathbf{x}}^*, \dot{\theta}^*$ are respectively the actual current end-effector's position and velocity and the joint angles' velocities. The numbers in parentheses refer to the corresponding equations in the text.

variables (end-effector velocity profiles for the velocity model, or end-effector positions, velocities and accelerations for the acceleration model) are extracted from the set of demonstrated trajectories and used to train a Gaussian Mixture Model (GMM) (see Table I). During reproduction, the trajectory is specified by a spring-and-damper dynamical system modulated by the GMM (see section III). The target is tracked by a stereo-vision system and is set to be the attractor point of the dynamical system. At each time step, the desired velocity computed by the model is then fed to a PID controller for execution. This does not hinder the online adaptation of the movement.

B. Velocity Model

The first way to encode a motion in a GMM, is to consider the velocity profile of the end-effector as a function of time $\dot{\mathbf{x}}(\mathbf{t})$. Thus, the input variable ζ is the time and the output variable ξ is the velocity, like in the following velocity model:

$$\dot{\mathbf{x}}^{\mathbf{m}} = \tilde{\mathcal{F}}_{\dot{\mathbf{x}}}(t) \tag{2}$$

In other words, the movement is modeled as a velocity profile, given by a function of time, which is learned as described in Table I. Here and henceforth, $\dot{\mathbf{x}}^{\mathbf{m}} \in \mathbb{R}^m$ is the end-effector velocity specified by the task model. $\tilde{\mathcal{F}}_{\dot{\mathbf{x}}}$ is obtained by applying (1) with the appropriate variables.

C. Acceleration Model

A second way of encoding a trajectory is to take as input the position $\mathbf{x}$ and velocity $\dot{\mathbf{x}}$, and as output the acceleration $\ddot{\mathbf{x}}$. The rationale of this is to consider a trajectory not as a function of time, but as the realization of a second-order dynamical system of the form:

$$\ddot{\mathbf{x}}^{\mathbf{m}} = \tilde{\mathcal{F}}_{\ddot{\mathbf{x}}}(\mathbf{x}, \dot{\mathbf{x}}). \tag{3}$$

Again, $\tilde{\mathcal{F}}_{\dot{\mathbf{x}}}$ is obtained by applying (1) with the appropriate variables. The velocity specified by the acceleration model is then given by

$$\dot{\mathbf{x}}^{\mathbf{m}} = \dot{\mathbf{x}} + \tau \tilde{\mathcal{F}}_{\ddot{\mathbf{x}}}(\mathbf{x}, \dot{\mathbf{x}}), \tag{4}$$

where τ is the time integration constant (set to 1 in this paper). Since the position $\mathbf{x}$ and velocity $\dot{\mathbf{x}}$ depend on the acceleration $\ddot{\mathbf{x}}$ at previous times, this representation introduces a feedback loop, which is not present in the representation given by (2).

III. Modulated Spring-and-Damper System

We now show how the task model described above is used to modulate a spring-and-damper dynamical system in order to enable a (possibly redundant) robotic arm with n joints to reproduce the task with sufficient flexibility. Although the modulation $\dot{\mathbf{x}}^{\mathbf{m}}$ is in end-effector space, it is advantageous (for avoiding singularity problems related to inverse kinematics of redundant manipulators) to consider the spring-and-damper dynamical system in joint angle variables:

$$\ddot{\theta}^{\mathbf{s}} = \alpha(-\dot{\theta} + \beta(\theta^{\mathbf{g}} - \theta)) \tag{5}$$

where $\theta \in \mathbb{R}^n$ is the vector of joint angles (or arm configuration vector). This dynamical system produces straight paths (in joint space) to the target $\theta^{\mathbf{g}}$, which acts as an attractor of the system. This guarantees that the robot reaches the target smoothly, despite possible perturbations.

The above dynamical system is modulated by the variable $\dot{\mathbf{x}}^{\mathbf{m}}$ given by the task model (2) or (4). In order to weigh the modulation, we introduce a modulation factor $\gamma \in \mathbb{R}_{[0\ 1]}$, which weighs the importance of the task model relatively to the spring-and-damper system. If $\gamma = 0$, only the spring-and-damper system is considered, and when $\gamma = 1$ only the task model is considered. In order to guarantee the convergence of the system to $\theta^{\mathbf{g}}$, γ has to tend to zero at the end of the movement. In the experiments described here, γ is given by:

$$\ddot{\gamma} = \alpha_\gamma(-\dot{\gamma} - \frac{1}{4}\alpha_\gamma\gamma) \quad \text{with } \gamma_0 = 1, \tag{6}$$

where γ_0 is the initial value of γ and $\alpha_\gamma \in \mathbb{R}_{[0\ 1]}$ is a scalar.

Since $\dot{\mathbf{x}}^{\mathbf{m}}$ lives in the end-effector space (and not in the joint space), the modulation is performed by solving the following constrained optimization problem.

$$\begin{aligned} \dot{\theta} = \quad & \underset{\dot{\theta}}{\operatorname{argmin}} \quad (1-\gamma)(\dot{\theta} - \dot{\theta}^{\mathbf{s}})^T \bar{\mathbf{W}}_\theta (\dot{\theta} - \dot{\theta}^{\mathbf{s}}) + \\ & \qquad \gamma(\dot{\mathbf{x}} - \dot{\mathbf{x}}^{\mathbf{m}})^T \bar{\mathbf{W}}_{\mathbf{x}} (\dot{\mathbf{x}} - \dot{\mathbf{x}}^{\mathbf{m}}) \qquad (7) \\ & \text{u.c.} \qquad \dot{\mathbf{x}} = \mathbf{J}\dot{\theta}, \qquad (8) \end{aligned}$$

where $\mathbf{J}$ is the Jacobian of the robot arm kinematic function $\mathbf{K}$ and $\bar{\mathbf{W}}_\theta \in \mathbb{R}^{n\times n}$ and $\bar{\mathbf{W}}_{\mathbf{x}} \in \mathbb{R}^{m\times m}$ are diagonal matrices necessary to compensate for the different scale of the $\mathbf{x}$ and θ variables. As a rough approximation, the diagonal elements of $\bar{\mathbf{W}}_{\mathbf{x}}$ are set to one and those of $\bar{\mathbf{W}}_\theta$ are set to the average distance between the robot base and its end-effector.

The solution to this minimization problem is given by [20]:

$$\dot{\theta} = \left(\mathbf{W}_\theta + \mathbf{J}^T\mathbf{W}_{\mathbf{x}}\mathbf{J}\right)^{-1}\left(\mathbf{W}_\theta\dot{\theta}^{\mathbf{s}} + \mathbf{J}^T\mathbf{W}_{\mathbf{x}}\dot{\mathbf{x}}^{\mathbf{m}}\right) \tag{9}$$

$$\text{where} \quad \mathbf{W}_\theta = (1-\gamma)\bar{\mathbf{W}}_\theta, \quad \mathbf{W}_{\mathbf{x}} = \gamma\bar{\mathbf{W}}_{\mathbf{x}}. \tag{10}$$

To summarize, the task is performed by integrating the following dynamical system:

$$\ddot{\theta}^{\mathbf{s}} = \alpha(-\dot{\theta} + \beta(\theta^{\mathbf{g}} - \theta)) \tag{11}$$

$$\dot{\theta} = \left(\mathbf{W}_\theta + \mathbf{J}^T\mathbf{W}_{\mathbf{x}}\mathbf{J}\right)^{-1}\left(\mathbf{W}_\theta\dot{\theta}^{\mathbf{s}} + \mathbf{J}^T\mathbf{W}_{\mathbf{x}}\dot{\mathbf{x}}^{\mathbf{m}}\right) \tag{12}$$

TABLE I

SUMMARY OF GAUSSIAN MIXTURE REGRESSION (GMR).

GMR is a method suggested by [19] for statistically estimating a function $\mathcal{F}_\xi(\zeta)$ given by a "training set" of N examples $\{(\zeta^i, \xi^i)\}_{i=1}^N$, where ξ^i is a noisy measurement of $\mathcal{F}_\xi(\zeta^i)$:

$$\xi^i = \mathcal{F}_\xi(\zeta^i) + \epsilon^i$$

(ϵ^i is the Gaussian noise). The idea is to model the joint distribution of the "input" variable ζ and an "output" variable ξ as a Gaussian Mixture Model. If we join those variables in a vector $\upsilon = [\zeta^T \xi^T]^T$, it is possible to model its probability density function as a mixture of K Gaussian functions

$$p(\upsilon) = \sum_{k=1}^{K} \pi_k \mathcal{N}(\upsilon; \mu_k, \mathbf{\Sigma}_k), \quad \text{such that} \quad \sum_{k=1}^{K} \pi_k = 1$$

where the $\pi_k \in [0\ 1]$ are the priors, and $\mathcal{N}(\upsilon; \mu_k, \mathbf{\Sigma}_k)$ is a Gaussian function with mean μ_k and covariance matrix $\mathbf{\Sigma}_k$:

$$\mathcal{N}(\upsilon; \mu_k, \mathbf{\Sigma}_k) = \left((2\pi)^d |\mathbf{\Sigma}_k|\right)^{-\frac{1}{2}} \exp\left(-\frac{1}{2}(\upsilon - \mu_k)^T \mathbf{\Sigma}_k^{-1} (\upsilon - \mu_k)\right),$$

where d is the dimensionality of the vector υ. The mean vectors μ_k and covariance matrices $\mathbf{\Sigma}_k$ can be separated into their respective input and output components:

$$\mu_k = [\mu_{k,\zeta}^T \ \mu_{k,\xi}^T]^T \qquad \mathbf{\Sigma}_k = \begin{pmatrix} \mathbf{\Sigma}_{k,\zeta} & \mathbf{\Sigma}_{k,\zeta\xi} \\ \mathbf{\Sigma}_{k,\xi\zeta} & \mathbf{\Sigma}_{k,\xi} \end{pmatrix}$$

The Gaussian Mixture Model (GMM) is trained using a standard E-M algorithm, taking the demonstrations as training data. The GMM computes a joint probability density function for the input and the output, so that the probability of the output conditioned on the input are GMM. Hence, it is possible, after training, to recover the expected output variable $\tilde{\xi}$, given the observed input variable ζ.

$$\tilde{\xi} = \tilde{\mathcal{F}}_\xi(\zeta) = \sum_{k=1}^{K} h_k(\zeta)\left(\mu_{k,\xi} + \mathbf{\Sigma}_{k,\xi\zeta}\mathbf{\Sigma}_{k,\zeta}^{-1}(\zeta - \mu_{k,\zeta})\right), \qquad (1)$$

where the $h_k(\zeta)$ are given by:

$$h_k(\zeta) = \frac{\pi_k \mathcal{N}(\zeta; \mu_{k,\zeta}, \mathbf{\Sigma}_{k,\zeta})}{\sum_{k=1}^{K} \pi_k \mathcal{N}(\zeta; \mu_{k,\zeta}, \mathbf{\Sigma}_{k,\zeta})}.$$

The tilde ($\tilde{}$) sign indicates that we are dealing with expectation values.

where $\mathbf{W_x}$ and $\mathbf{W}_\theta$ are given by (6) and (10), and $\dot{\mathbf{x}}^\mathbf{m}$ is given either by (2) (velocity model) or by (4) (acceleration model). Integration is performed using a first-order Newton approximation ($\dot{\theta}^\mathbf{s} = \dot{\theta} + \tau\ddot{\theta}^\mathbf{s}$).

Since the target location is given in cartesian coordinates, inverse kinematics must be performed in order to obtain the corresponding target joint angle configuration which will serve as input of the spring-and-damper dynamical system. In the case of a redundant manipulator (such as the robot arm used in the following experiments) the desired redundant parameters of the target joint angle configuration can be extracted from the demonstrations. This is done by using the GMR technique described in Table I to build a model of the final arm configuration as a function of the target location.

Using an attractor system in joint angle space has the practical advantage of reducing the usual problems related to end-effector control, such as joint limit and singularity avoidance. Equation 9, which is a generalized version of the Damped Least Squares inverse [21] [22], is a way to simultaneously control the joint angles and the end-effector, imposing soft constraints on both of them. It is thus different than optimizing the joint angles in the null space of the kinematic function.

IV. EXPERIMENTS

A. Setup

We validate and compare the systems described in this paper on two experiments. The first experiment involves a robot putting an object into a box and the second experiment consists in reaching and grasping for an object. Those experiments were chosen because (1) they can be considered as simple goal-directed tasks (for which the system is intended), (2) they are tasks commonly performed in human environments and (3) they presents a clear success or failure criterion.

All the experiments presented below are performed with a Hoap3 humanoid robot acquired from Fujitsu. This robot has four back-drivable degrees of freedom (dof) at each arm. Thus, the robot arms are redundant, as we do not consider end-effector orientation. The robot is endowed with a stereo-vision system enabling it to track color blobs. A color patch is fixed on the box and on the object to be grasped, enabling their 3D localization. Pictures of the setup are shown in Fig. 2.

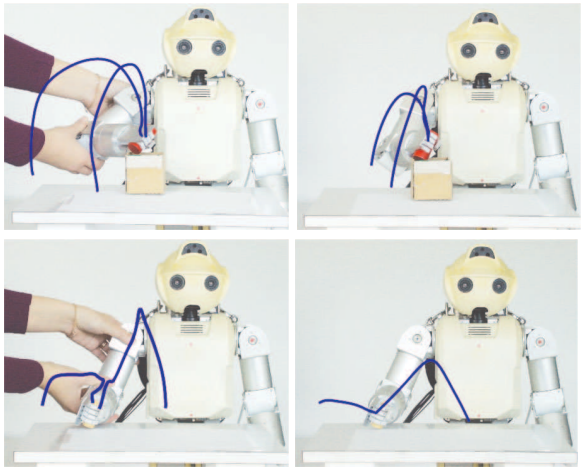

Fig. 2. The setup of the experiments. The top pictures show the first task and the lower picture sow the second task Left: a human operator demonstrates a task to the robot by guiding its limbs. Right: the robot performs the task, starting from different initial positions.

1) Preprocessing: During the demonstrations, the robot joint angles were recorded and the end-effector positions were computed using the arm kinematic function. All recorded trajectories were linearly normalized in time ($T = 500$ time steps) and Gaussian-filtered to remove noise. The number of Gaussian components for the task models were found using the Bayesian Information Criteria (BIC) [23], and the parameter values used were $\alpha_\gamma = 0.06$, $\alpha = 0.12$ and $\beta = 0.06$.

B. Putting an object into a box

1) Description: For this task, the robot is taught to put an object into the box (see Fig.2). In order to accomplish the task, the robot has to avoid hitting the box while performing the movement and must thus first reach up above the box and

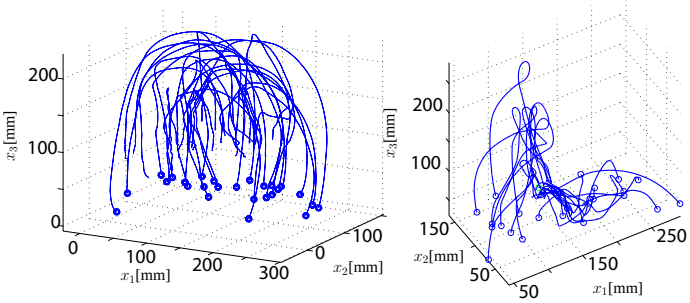

Fig. 3. The demonstrated trajectories for the box task (left) and the grasping task (right). Circles indicate starting positions.

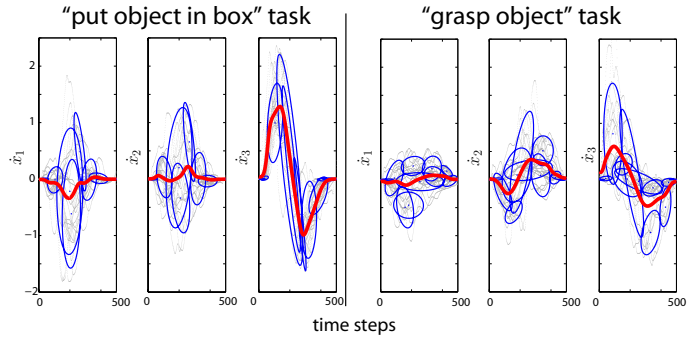

Fig. 4. The velocity models for both tasks. The dots represent the training data, the ellipses the Gaussian components and the thick lines the trajectory obtained by GMR alone. The thick lines show that, for the first task, the horizontal components $\dot{x}_1$ and $\dot{x}_2$ are averaged out by the model, but the vertical component $\dot{x}_3$ shows a marked upward movement. For the second task, all components are almost averaged out.

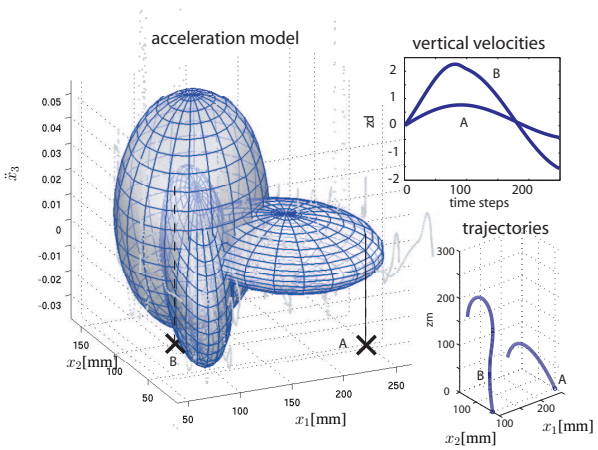

Fig. 5. In the center, the acceleration model for the second task. The ellipsoids show the Gaussian components at twice their standard deviation. Only three projections (out of nine) are shown. The vertical acceleration strongly depends on the position in the horizontal plane. On the lower right, two trajectories encoded by this model but starting from different positions A and B (indicated by the crosses) are shown. The corresponding vertical velocity profiles appear on the upper right. They differ significantly, as the model is not homogeneous across the horizontal plane.

then down to the box. A straight line reaching will in general cause the robot to hit the box while reaching and thus fail.

2) Training: A set of 26 kinesthetic demonstrations were performed, with different initial positions and box locations. The box was placed on a little table. Thus its location only varies in the horizontal plane. Similarly, the initial position of the object (and thus of the end-effector) lied on the table. The set of demonstrated trajectories is depicted in Fig. 3, left. The velocity models trained on this data are shown in Fig. 4, left.

C. Reach and Grasp

1) Description: In order to accomplish this task, the robot has to reach and correctly place its hand to grasp a chess piece. In other words it has to place its hand so that the chess piece stands between its thumb and its remaining fingers, as shown in Fig. 7, left. This figure illustrates that the approaching the object can only be done in one of two directions: downward or forward. This task is more difficult than the previous one, as the movement is more constrained. Moreover, a higher precision is required on the final position, since the hand is relatively small.

2) Training: A set of 24 demonstrations were performed starting from different initial positions located on the horizontal plane of the table. The chess piece remained in a fixed location. Depending on the initial position, the chess piece was approached either downward or forward (as illustrated on Fig. 7). The set of demonstrations is represented in Fig. 3, right. The resulting velocity model is shown in Fig. 4, right. One can notice that there is no velocity feature that is common to all demonstrated trajectories. The acceleration model is shown in Fig. 5. This model captures well the fact that the vertical acceleration component depends on the position in the horizontal plane.

D. Results

Endowed with the system described above, the robot is able to successfully perform both tasks. For the first task, both the velocity and the acceleration models can produce adequate trajectories (see Fig. 6, left for examples). The system can adapt its trajectory online if the box is moved during movement execution (see Fig. 6, right). For the second task, examples of resulting trajectories are displayed in Fig. 7, right. In order to evaluate the generalization abilities of the systems, both tasks were executed from various different initial positions arbitrarily chosen on the horizontal plane of the table, and covering the space reachable by the robot. Fig. 8 shows the results and starting positions for both experiments. For the box experiment (left), the velocity model was successful for 22 out of the 24 starting locations (91%). The two unsuccessful trials, indicated by empty circles, correspond to initial positions close to the work space boundaries. The acceleration model was successful for all trials (100%).

For the chess piece experiment (Fig. 8, right), the velocity model was successful for 5 out of 21 (24%) trials whereas the acceleration model was successful for 18 trials (86%). This performance gap is due to the fact that this task does not require a fixed velocity modulation. The adequate modulation depends on the position. This position-dependent modulation can be captured by the acceleration model, but not by the velocity model. As illustrated in Fig. 5, the acceleration model

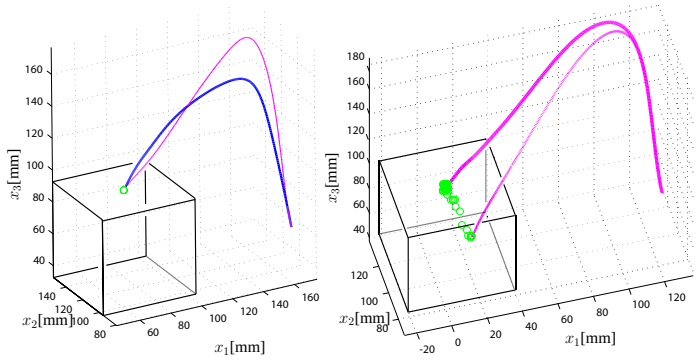

Fig. 6. Left: end-effector trajectories of the robot putting the object into the box. The thin line corresponds to the velocity model and the thick line corresponds to the acceleration model. Right: online trajectory adaptation to a target displacement using the velocity model. The circles indicate to location of the box, as tracked by the stereo-vision system. The thick line shows the produced trajectory and the thin line shows the original trajectory if the box remained unmoved. Similar results were obtained with the acceleration model.

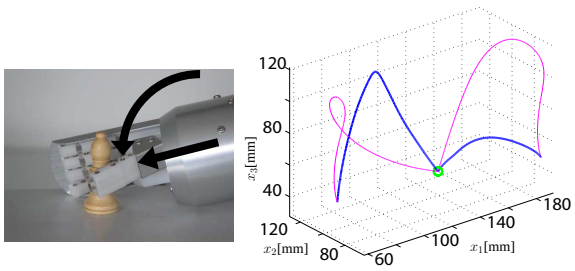

Fig. 7. Left: the chess piece to be grasped. For a successful grasp, the robot has to approach it as indicated by the arrows. Right: resulting trajectories for the grasping task, starting from two different initial positions. The acceleration model (thick lines) adapts the modulation to the initial position, while the velocity model (thin lines) starts upward in both cases. The trajectory produced by the velocity model and starting left of the target is not successful.

is able to produce different velocity profiles, depending on the starting position and is thus more versatile than the velocity model.

V. Discussion

Our results show that the framework suggested in this paper can enable a robot to learn constrained reaching tasks from kinesthetic demonstrations, and generalize them to different initial conditions. Using a dynamical system approach allows to deal with perturbations occurring during the task execution. This framework can be used with various task models and has been tested for two of them, the velocity model and the acceleration model. The results indicate that the velocity model is too simplistic if the task requires different velocity profiles when starting from different positions in the workspace. The acceleration model, which models the task as a dynamical system rather than as a trajectory, is more sophisticated and can model more constrained movements. However, it may fail to provide an adequate trajectory when brought away from the demonstrations in the phase space $(\mathbf{x}, \dot{\mathbf{x}})$. Other regressions techniques, such as LWR, could also be used. But if there are inconsistencies across demonstrations, simple averaging may fail to provide

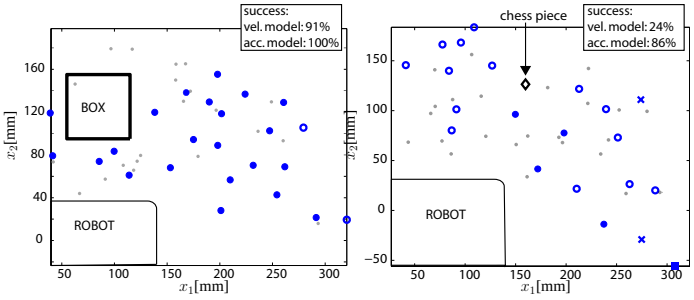

Fig. 8. The robustness to initial end-effector position for both tasks. The plots represent top views of the first (right) and second (left) experiment. The filled markers (circles or squares) indicate all initial positions for which the velocity model was successful. The circles (filled and non-filled) indicate all initial positions for which the acceleration model was successful. The crosses indicate initial end-effector position, for which both models failed. The dots indicate the starting positions of the training set.

adequate solutions.

In its present form, the modulation factor between the dynamical system and the task model (γ) is not learned. Learning it from the demonstrations is likely to further improve the performance of the system, especially for tasks requiring a modulation at the end of the movement. It would also be desirable to have a system that extracts the relevant variables, and automatically selects the adequate model. A first step in this direction has been taken in [24], where a balance between different sets of variables is achieved.

Of course, the adequacy of this framework is restricted to relatively simple tasks, such as those described in the experiments. More complicated tasks, such as obstacle avoidance in complex environments or stable grasping of particular objects require a detailed model of the environment and more elaborate planning techniques. The tasks considered for this framework are those that cannot be accomplished by simple point-to-point reaching, but still simple enough to avoid the complete knowledge of the environment. But this framework could be extended to learn more complicated tasks. In a first step in this direction, [18] investigates how Reinforcement Learning can deal with obstacle avoidance.

References

[1] A. Billard, S. Calinon, R. Dillmann, and S. Schaal, "Robot programming by demonstration," in *Handbook of Robotics*, B. Siciliano and O. Khatib, Eds. Springer, 2008.

[2] R. Burridge, A. Rizzi, and D. Koditschek, "Sequential composition of dynamically dexterous robot behaviors," *International Journal of Robotics Research*, 1999.

[3] J. Ponce, S. Sullivan, A. Sudsang, J.-D. Boissonnat, and J.-P. Merlet, "On computing four-finger equilibrium and force-closure grasps of polyhedral objects," *International Journal of Robotics Research*, vol. 16, no. 1, pp. 11–35, 1997.

[4] K. Lynch and M. Mason, "Dynamic manipulation with a one joint robot," in *IEEE International Conference on Robotics and Automation (ICRA '97)*, 1997.

[5] I. Iossifidis and G. Schöner, "Autonomous reaching and obstacle avoidance with the anthropomorphic arm of a robotic assistant using the attractor dynamics approach," in *Proceedings of the IEEE International Conference on Robotics and Automation*, 2004, pp. 4295–4300.

[6] C. Goldfeder, P. Allen, C. Lackner, and R. Pelossof, "Grasp planning via decomposition trees," in *Proceedings of the IEEE International Conference on Robotics and Automation*, 2007, pp. 4679–4684.

[7] R. Platt, A. Fagg, and R. Grupen, "Manipulation gaits: Sequences of grasp control tasks," in *Proceedings of the International Conference on Robotics and Automation*, 2004, pp. 801–806.
[8] S. Ekvall and D. Kragic, "Interactive grasp learning based on human demonstration," in *Proceedings of the International Conference on Robotics and Automation*, 2004, pp. 3519–3524.
[9] A. Ijspeert, J. Nakanishi, and S. Schaal, "Movement imitation with nonlinear dynamical systems in humanoid robots," in *Proceedings of the IEEE International Conference on Robotics and Automation*, 2002, pp. 1398–1403.
[10] W. Ilg, G. Bakir, J. Mezger, and M. Giese, "On the representation, learning and transfer of spatio-temporal movement characteristics," *International Journal of Humanoid Robotics*, pp. 613–636, 2004.
[11] A. Shon, J. Storz, and R. Rao, "Towards a real-time bayesian imitation system for a humanoid robot," in *Proceedings of the IEEE International Conference on Robotics and Automation*, 2007, pp. 2847–2852.
[12] O. Jenkins, G. González, and M. Loper, "Tracking human motion and actions for interactive robots," in *Proceedings of the Conference on Human-Robot Interaction (HRI07)*, 2007, pp. 365–372.
[13] T. Inamura, I. Toshima, H. Tanie, and Y. Nakamura, "Embodied symbol emergence based on mimesis theory." *International Journal of Robotics Research*, vol. 23, no. 4-5, pp. 363–377, 2004.
[14] D. Grimes, D. Rashid, and R. Rao, "Learning nonparametric models for probabilistic imitation," in *Advances in Neural Information Processing Systems (NIPS 06)*, 2006.
[15] K. Ogawara, J. Takamatsu, H. Kimura, and K. Ikeuchi, "Extraction of essential interactions through multiple observations of human demonstrations," *IEEE Trans. Ind. Electron.*, vol. 50, pp. 667–675, 2003.
[16] R. Dillmann, "Teaching and learning of robot tasks via observation of human performance," *Robotics and Autonomous Systems*, no. 2,3, pp. 109–116, 2004.
[17] C. Campbell, R. Peters, R. Bodenheimer, W. Bluethmann, E. Huber, and R. Ambrose, "Superpositioning of behaviors learned through teleoperation," *IEEE Transactions on Robotics*, 2006.
[18] F. Guenter, M. Hersch, S. Calinon, and A. Billard, "Reinforcement learning for imitating constrained reaching movements," *RSJ Advanced Robotics*, vol. 21, no. 13, pp. 1521–1544, 2007.
[19] Z. Ghahramani and M. Jordan, "Supervised learning from incomplete data via an em approach," in *Advances in Neural Information Processing Systems 6*, J. Cowan, G. Tesauro, and J.Alspector, Eds. Morgan Kaufmann Publishers, 1994.
[20] A. Billard, S. Calinon, and F. Guenter, "Discriminative and adaptive imitation in uni-manual and bi-manual tasks," *Robotics and Autonomous Systems*, vol. 54, no. 5, pp. 370–384, 2006.
[21] C. Wampler, "Manipulator inverse kinematic solutions based on vector formulations and damped least-squares methods," *IEEE Transactions on Systems, Man and Cybernetics, Part C*, vol. 16, no. 1, pp. 93–101, 1986.
[22] Y. Nakamura and H. Hanafusa, "Inverse kinematics solutions with singularity robustness for robot manipulator control," *ASME Journal of Dynamic Systems, Measurement, and Control*, vol. 108, pp. 163–171, 1986.
[23] G. Schwarz, "Estimating the dimension of a model," *Annals of Statistics*, vol. 6, 1978.
[24] S. Calinon, F. Guenter, and A. Billard, "On learning, representing and generalizing a task in a humanoid robot," *IEEE Trans. Syst., Man, Cybern. B*, vol. 37, no. 2, pp. 286–298, 2007.

Imitation and Focus of Attention: Technical Report

A. Just [a] A. Billard [a] L. Craighero [b] A. D'Ausilio [b] A. Oliynyk [b] L. Fadiga [b,c]

[a] *Learning Algorithms and Systems Laboratory, Ecole Polytechnique Fédérale de Lausanne, 1015 Lausanne. Switzerland*

[b] *Section of Human Physiology, University of Ferrara, 44100 Ferrara. Italy*

[c] *The Italian Institute of Technology, 16163 Genova. Italy*

Abstract

Imitation plays an important role in the development of human beings. During childhood, it provides means to learn new motor skills. During adulthood, imitation helps the acquisition of several skills without the time-consuming process of trial-and-error learning. Several theories have been proposed to explain the process of imitation, but the question remains opened. The present study investigates the behavior of normal subjects during imitation of simple movements. Possible correlation between quality of imitation and attention behavior will be studied to underline a possible correlation.

Key words: imitation, goal-direct imitation, specular imitation, anatomic imitation, VITE model, Lagrange optimization, gesture modeling

1 Introduction

Humans were thought to learn to imitate over the first years of life. But work from Meltzoff [Meltzoff and Moore, 1977, 2002] has shown that even newborns can imitate body and facial movements at birth. Questions that arise from the study of imitation are related to its underlying mechanisms. Meltzoff and Moore [Meltzoff and Moore, 1997] propose the Active Intermodal Mapping (AIM) to explain facial imitation in infants. AIM hypothesizes that the perception and production of actions can be represented within a common framework. This common framework, or "supramodal" representation, permits newborns to perform a matching process between their own movements and the ones they see. An infant's own movements then provide some

proprioceptive information that can be compared to the visual target action. Furthermore, AIM supposes a goal-directed matching process. Indeed, infants will attempt novel means to reach similar actions, e.g. to obtain the same effect as a tongue protruding to the side, infants will use a straight protruding tongue associated with head rotated to the side.

To explain imitation, the direct matching approach has also been proposed. This mechanism supposes that the observed action is directly linked to our motor representation of the same action. The direct matching hypothesis is closely related to the discovery of mirror neurons. The mirror system provides a natural link between action understanding and imitation. Mirror neurons were first discovered in monkeys' brain. In area F5 of the monkey premotor cortex [Rizzolatti et al., 1996, Rizzolati et al., 2002] neurons were found that discharge both when the monkey performs an action and when he observes a similar action made by conspecies or by the experimenter. These neurons discharge during particular goal-directed hand movements such as grasping, holding or manipulating some food or object.Evidence suggests that area F5 in monkeys' brain correspond to an observation/execution matching system.

The direct matching hypothesis for imitation in humans supposes the existence of a mechanism similar to mirror neurons in monkeys. It supposes the existence of a mechanism directly matching the observed action onto an internal motor representation of that action. The direct matching hypothesis predicts that the areas where matching occurs must contain neurons that discharge during action execution both when observing and executing the action. Using functional magnetic resonance imaging, the authors in [Iacoboni et al., 1999] showed an activation of the left frontal operculum (area 44) and the right anterior parietal cortex (PE/PC). These findings indicate that these areas of the human brain have an imitation mechanism similar to mirror neurons found in monkeys, as postulated by the direct matching hypothesis. The authors proposed that the inferior frontal area describes the precise details of the movement. In contrast, the parietal lobe area codes the precise kinesthetic aspects of the movement.

Recent findings in the field of imitation do not fit with previously presented theories of imitation. The work by Bekkering and colleagues [Bekkering et al., 2000, Wohlschläger et al., 2003] show that children's behavior when imitating does not always follow a direct visual-to-motor mapping between perceived and imitated movements. The new theory they propose, called the goal-directed (GOADI) theory of imitation, hypothesizes that imitation is guided by cognitively specified goals. When observing and executing an action, imitators do not imitate the observed movement as a whole, which would be the expected outcome with previous theories of imitation, but instead decompose the action into separate aspects. These aspects are following a predefined hierarchy. At the top of the pyramid can be found the goal of the action. All

the other aspects of the movement are seen as sub-goals, thus of less imitative importance. In the presence of a target or object (transitive actions), experiments show that movements seem to be imitated correctly with respect to the goal, but the movement itself is frequently ignored. When dealing with intransitive action, i.e. when there is no target/object at the core of the movement, the movement itself tends to become the main goal of the action. In that case, the particular kinematics of the movement are precisely reproduced.

In real life, children show a strong tendency to imitate actions as if looking in a mirror (specular mode) rather than with the anatomically congruent hand (anatomic mode). Furthermore, most studies on imitation have used mirror imitation and very few experiments have been conducted to test whether a difference exists between mirror and non-mirror imitation.Previous study [Iacoboni et al., 1999] shows patterns activity in the frontal opercular and posterior parietal regions for both observed and executed actions. Koski et al. [Koski et al., 2003] show that the activity in the frontal opercular and posterior parietal regions varies as a function of the type of imitation, specular versus anatomic mode, being performed. Their results show different neuron activity in frontoparietal regions during different forms of imitative behavior. It enhances the importance of mirror neurons for imitating in the specular mode. Franz et al. [Franz et al., 2007] provide further results on comparison of specular and anatomic modes for imitation. They hypothesize that in imitative tasks involving both hands, both specular mode and anatomic mode are in competition, and the shift from one type of imitation to the other depends on the task, situation, and stimuli as well as the instructions given to the imitator. They also showed that when using mirror imitation, the goal of the action (the final target) is at the top of the hierarchy of movement aspects. These findings provide more grounding for the GOADI theory of imitation [Bekkering et al., 2000], but they also show that this tendency is inverted when dealing with anatomic imitation. In this condition, the use of the anatomically correct hand tends to take the first place in the hierarchy of imitation goals.Overall, their findings suggest that specular and anatomic imitation are two distinct processes and in consequence the two modes may obey different principles.

2 Materials and Methods

2.1 Subjects

Nine healthy subjects (4 females, 5 males, mean age 25 $\pm$ 4) volunteered to perform a one-handed task consisting of point-to-point motions. All subjects were right-handed (Edinburgh Handedness test [Oldfield, 1971]). They were all naive regarding the purpose of the experiment. They reported no history

of neurological or musculo-skeletal deficits. All had normal or corrected to normal vision.

2.2 Procedure

Subjects were comfortably sitting on a chair in front of a table. They were asked to maintain a steady trunk position all along the recording session. Each hand movement started in the same rest position, with the right forearm lying on the table, and it being perpendicular to the trunk. Subject's left arm was placed under the table and they were asked not to use it during experiments. They were facing the demonstrator who had both arm placed on the table. Figure 1 presents the set-up with the experimenter, on the right, showing a movement to the subject, on the left.

Fig. 1. Experimenter (on the right) showing a movement to reproduce to the subject (on the left).

Subjects were shown by the experimenter a series of movement to reproduce. There were two conditions. In the first condition, movements were directed towards an object placed 30 cm away from the subject, in the sagittal plane (Figure 2). Both the subject and experimenter had a similar object placed in front of them at the same time. In the second condition, subjects had to reach in front of them and land their hand palm-down on the table. No location on the table was specified in this second condition. We refer to these two conditions respectively as transitive (Trans) and intransitive (Intrans) movements in the rest of the paper.

For each condition, the subjects were shown two variants of the movements. In the first variant (so-called "Elb"), the experimenter was exaggeratedly elevating the elbow throughout the motion. In the second variant (so-called "Norm"), the experimenter was performing the motion in way as natural as possible. Movements performed by the experimenter were thus of four types: intransitive with normal kinematics (**Intrans Norm**), intransitive with an exaggerated elevation of the elbow (**Intrans Elb**), transitive with normal kinematics (**Trans Norm**) and transitive with an exaggerated elevation of

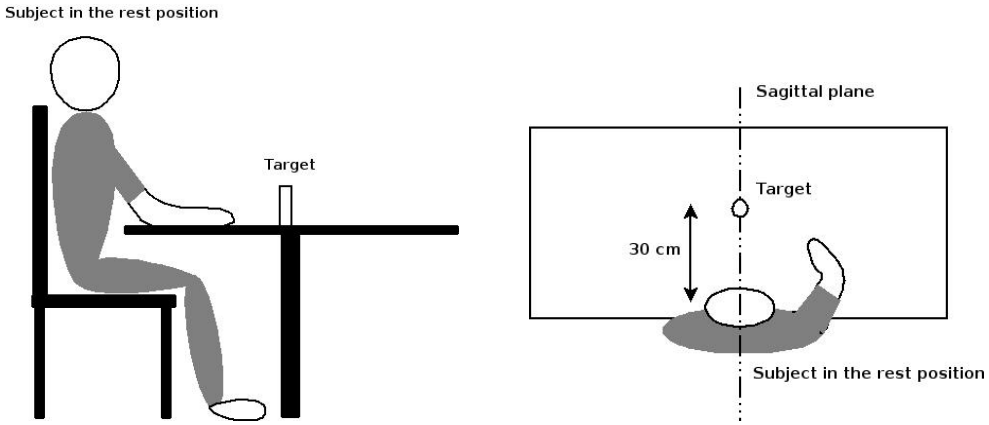

Fig. 2. Left: Set-up seen from the right side with the subject in the rest position. Right: upper view of the set-up with the position of the target when performing transitive motions

the elbow (**Trans Elb**). For transitive actions, two objects were placed on the table, one for the subject, the other one for the experimenter. The objects were similar for both the subject and experimenter.

Intrans Norm Intrans Elb Trans Norm Trans Elb

Fig. 3. Snapshots of the four gesture types. From left to right: Intransitive action with normal kinematics and with an exaggerated elevation of the elbow. Transitive movement with normal kinematics and with an exaggerated elevation of the elbow. One can see that for the "Elb" variant the elbow position is always higher than for movements performed with normal kinematics for both the "Intrans" and "Trans" conditions.

Subjects were shown a series of 128 movements (Table 1). They were explicitly told to reproduce the movement as soon as possible once the experimenter has shown them the movement. If the subject had questions about how to reproduce the movements, they were just told to do it the way they thought would be the most suitable to reproduce the movement.

Subjects	Movements per session	Recording sessions per subject
9	128	1

Table 1
Statistics of the database.

The experiment was decomposed in three distinct phases. In the first phase, the experimenter showed the movements only with the right hand. In the sec-

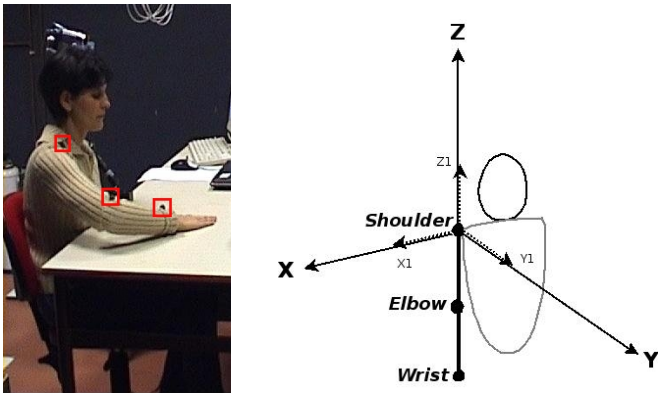

Fig. 4. Left: subject wearing markers on the right arm (markers are surrounded by red squares). Right: shoulder-centered frame of reference.

ond phase, both right and left hand were used. As the subjects was asked to perform movements only with the right hand, some confusion occured at that point during experiment. When the experimenter first showed movements with the left hand, subjects wanted also to switch hand to reproduce the movement. As they were told to use only the right hand, they asked for additional information about what to do. They were told to reproduce the movement with their right hand and they were reminded to always use their right hand in the remaining of the experiment. In the third and last phase, the experimenter again used only the right hand to perform the motions. These phases are conceptually distinct in the design of the experiment but had no incidence on the course of the experiment. In each phase, the experimenter was showing the four motion types. The detailed scenario of the experiment is presented in Appendix A. Subject's gaze data were also recorded during the experiment.

2.3 Data acquisition

The trajectories in space of the shoulder, elbow and wrist were recorded by using kinematics recording system formed by three ProReflex MCU1000 cameras (QUALISYS AB, Sweden) detecting the 3D position of infrared reflecting markers (n=4 for the subject and n=6 for the experimenter) positioned on the left and right shoulders, right elbow and right wrist for the subject and experimenter, as well as left elbow and left wrist for the experimenter. The position of the markers was recorded at a frequency of 200 Hz during the execution of the movements. Figure 4 presents one subject wearing the markers as well as the shoulder-centered frame of reference used in the following of the paper to calculate wrist and elbow trajectories.

Eye movements of the subject were recorded using a Tobii X50 eye tracker.

2.4 Data analysis

All analyzes were performed using the Qualisys Track Manager (QUALISYS AB, Sweden) and ClearView 2.5.1, plus custom software written in Matlab (Mathworks, Natick, MA). Analysis was done solely on the reaching phase of each movement (from the rest position to the target location in the case of transitive gestures, and from the rest position to the hand placement on the table in from of the subject for intransitive movements). Data were first segmented manually to remove any irrelevant movement prior to the onset of the reaching movement. We used only unfiltered raw values.
In order to analyze the gaze data, we decomposed the scene area into 4 main zones: Face, Right Arm, Left Arm and Center Region. The Center Region goes from the target position on the table to the hand not moving during the movement. Figure 5 presents the four areas.

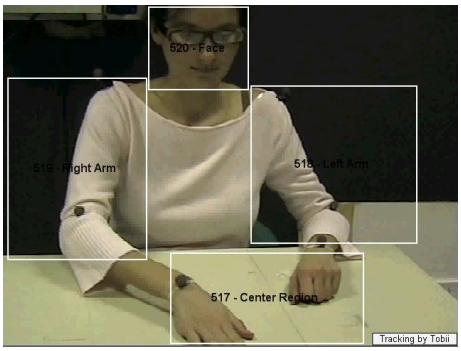

Fig. 5. Areas defined for the focus of attention of the subject while the experimenter is demonstrating a movement.

Fixation analysis was performed with a fixation radius of 30 pixels and a minimum fixation duration of 100 ms.

3 Results

3.1 Evolution of the elbow raise across phases

The quality of imitation can be assessed at two different levels. Firstly, the reproduction of the goal of the movement, i.e. reaching for an object (Trans) versus place the palm-down on the table (Intrans) is taken into account. Secondly, we can study the reproduction of the kinematic features of the movements. All subjects reproduced perfectly the change in condition of the movements (Intrans versus Trans). We can thus say that all subjects reproduced very well this characteristics of the motions during all three phases of the experiment.

None of them performed an intransitive motion when a transitive one was demonstrated and vice-versa. The presence or absence of the object was an obvious characteristic of the motion and thus it was very difficult to mistake one motion condition for the other.
The reproduction of the kinematic features of the movements in the first phase of the experiment shows two main categories of subjects. The first category includes Subjects 1 and 2 who already reproduce the two motion variants. The remaining subjects belong the the second category. These subjects poorly reproduce the exaggerated raise of the elbow in the Elb variant. Figure 6 presents the mean raise of the elbow for the Norm and Elb variants of the movements of the subject and experimenter for the Phase 1 of the experiment. On the left graph, the difference between Norm and Elb movements is well defined as the mean values of the elbow raise for the subject and experimenter are comparable. Conversely in the graph on the right, mean value for the Norm and Elb movements reproduced by the subjects are equal, thus not showing any difference between the two motion variants.

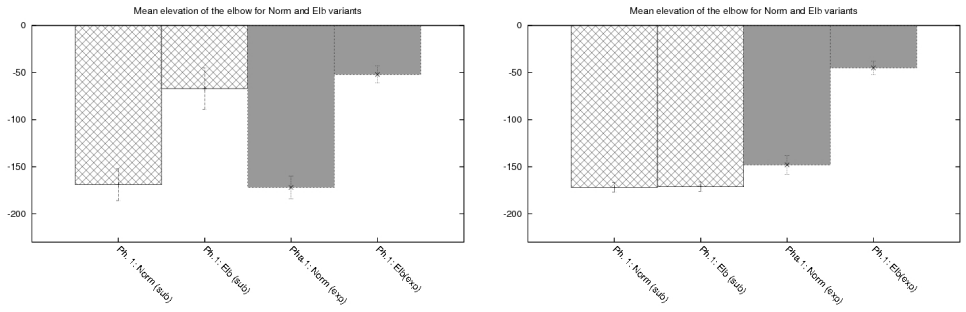

Fig. 6. Mean value for the raise of the elbow for Norm and Elb movements for both the subject and experimenter during Phase 1. On the left: subject reproducing the different motion types accurately. On the right: subject poorly reproducing the kinematic features of the movements

These results thus show that subjects have not equal imitation capabilities. Results in Phase 1 demonstrate that the fine reproduction of motion is inherently different from one subject to the other one.

We hypothesize that an unusual event can modify the reproduction capacities of the subjects. In Phase 2 of the experiment, we thus introduced an unusual event. In this phase, the experimenter switches between hands to show the movements to the subject. Subjects 1 and 2, who were already reproducing the exaggerated elevation of the elbow in Phase 1, are still showing strong imitation skills. For all the other subjects, an improvement is visible in Phase 2. Figure 7 shows the evolution of the mean raise of the elbow across the two phases for two different subjects. The graph on the left shows a subject performing well on both Phases 1 and 2 of the experiment. The other graph demonstrates a dramatic improvement in the reproduction of the reproduction of the Elb variant of the movements.

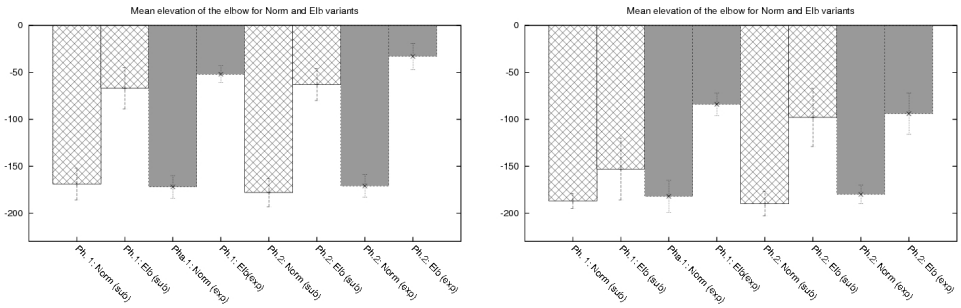

Fig. 7. Mean value for the raise of the elbow for Norm and Elb movements for both the subject and experimenter during Phases 1 and 2. On the left: subject reproducing the different motion types accurately across the two phases . On the right: subject poorly reproducing the kinematic features of the movements during Phase 1 but showing some improvement in Phase 2.

This improvement in the reproduction of the kinematic features of the movements lasts until the end of the experiment (Figure 8), except for Subject 8 for whom the improvement is visible only during Phase 2.

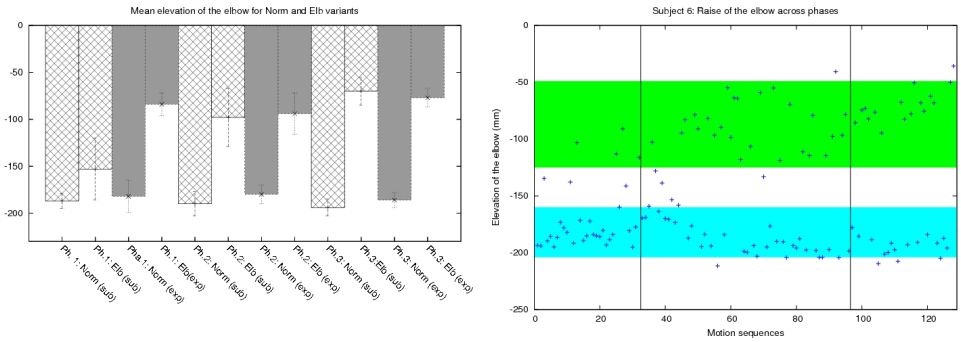

Fig. 8. Left: comparison of the mean raise of the elbow for the Norm and ELb movements for the subject (in light gray) and the experimenter (in dark gray). The evolution of the raise of the elbow is shown separately for each phase of the experiment. Right: Each dot corresponds to a single motion performed by the subject. The blue area corresponds to the range of Norm movements shown by the experimenter. The green ares corresponds to the Elb movements. The boundaries correspond to the mean value of the raise of the elbow plus or minus two standard deviations.

The Pearson coefficient [1] between the raise of the elbow of the experimenter and subject (Table 2) shows that a strong correlation exists between movements performed by the experimenter and movements reproduced by Subjects 1 and 2 ($\rho >= 0.9$).

[1] The Pearson coefficient is the sum of the products of the normalized values of the two measures divided by the degree of freedom. The Pearson coefficient ranges from +1 to -1. If $\rho = 0$, then there is no linear relationship between the two variables. On the contrary, if $|\rho| = 1$, then there is a perfect linear relationship between the two variables.

	Correlation ρ			
Subject	Total	Phase 1	Phase 2	Phase 3
Sub.1	0.96	0.93	0.94	0.95
Sub.2	0.90	0.92	0.85	0.93
Sub.3	0.80	0.73	0.80	0.85
Sub.4	0.44	0.10	0.46	0.78
Sub.5	0.82	0.76	0.83	0.86
Sub.6	0.81	0.64	0.81	0.94
Sub.7	0.54	0.33	0.64	0.62
Sub.8	0.56	0.60	0.58	0.51
Sub.9	0.81	0.77	0.85	0.84

Table 2
Pearson coefficient between the raise of the elbow of the experimenter and subject.

Furthermore, the evolution of the Pearson coefficient along the three phases of the experiment shows an increase of its value in Phase 2 for most of the subjects.

If we now compare the reproduction of movements in Phases 1 and 3 of the experiment, results show that an improvement of the reproduction of kinematic features by the subject. These results

These results show that an unusual event is able to modify the imitation state of the subject. In our case, the goal of this unusual event was to attract the attention of the subject on the hand of the experimenter. Results showed that this has also improved its capacities to reproduce accurately the kinematic features of the movements described in this paper.

3.2 Focus of attention

Figure 9 presents the percentage of fixation time subjects spend on the area of the arms of the experimenter.

From Phase 1 to Phase 2 of the experiment, the fixation time spent on the arm regions (Right Arm and Left Arm) increases for every subject. This shows that the unusual event introduced in Phase 2 has an effect on the attention focus, attracting the subjects gaze on the arms of the experimenter. We have shown in the previous Section that the unusual event introduced in Phase 2 had a positive effect on the reproduction of the kinematic features of the movements. This improvement may be due to this switch in the attention pattern that occurs during Phase 2.

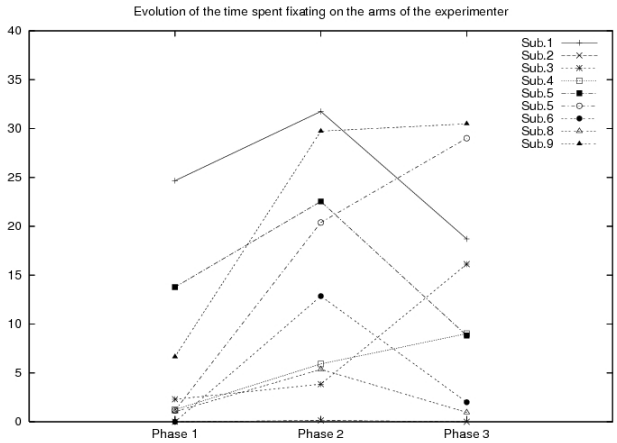

Fig. 9. Evolution of the percentage of fixation time spent on the arms of the experimenter for each subject and each phase of the experiment.

The behavior of Subject 2 is an outlier as the fixation time spent on the Right Arm and Left Arm area is close to zero. Most of the fixation points are localized in the Center Region (Figure 10).

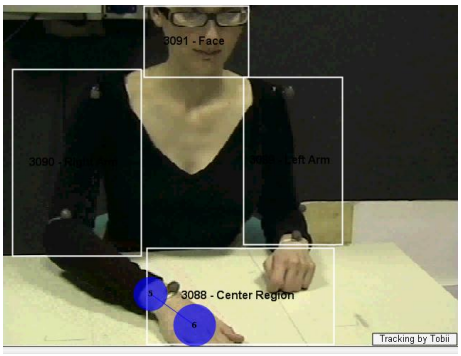

Fig. 10. Blue dots correspond to the focus points during an intransitive movement with normal kinematics (Intrans Norm) for Subject 2.

A thiner analysis of the fixation points in the Center Region shows that most of the fixation points are localized on the arm/wrist.

4 Discussion

- Unusual event implies a change in the behavior of the subject as the reproduction of kinematic features improves in Phase 2 of the experiment.
- Unusual event also implies a modification of the gaze of the subject as the time spent fixating the arms of the experimenter increases.
- The displacement of the focus of attention is linked to the quality of the reproduction of the kinematic features of the demonstrated motions.

A Scenario of the Recordings

The recordings can be decomposed into three parts. In the first and last part, the demonstrator is using only her right hand to perform the movements whereas in the middle part, both right and left hands are used to perform the actions. The first part consists of 32 gestures, the second of 64 gestures and the last part of 32 gestures again. We use the following notation: R for right hand, L for left hand, TR for transitive action and INT for intransitive, n means with normal kinematics and e are gestures performed with an abnormal elevation of the elbow.

Phase 1: R TR e - R INT n - R TR e - R INT n - R TR n - R INT n - R TR e - R INT e - R INT e - R INT n - R TR e - R TR n - R TR e - R INT e - R TR n - R TR n - R INT e - R INT n - R INT n - R TR n - R INT e - R TR n - R INT n - R INT e - R TR e - R TR n - R INT e - R TR e - R INT n - R TR n - R INT e - R INT e.

Phase 2: R INT n - L INT n - L TR e - L TR e - R INT e - R INT n - R TR e - R INT n - L TR n - L INT e - L TR n - R TR e - R TR e - R INT e - R INT n - L INT n - L INT e - R INT e - R TR n - L TR n - L INT e - L INT n - R INT e - L TR n - L INT e - R TR n - L TR e - R INT e - L INT e - R INT e - R TR e - L TR n - R TR n - L TR e - R TR n - L TR n - R INT e - L TR e - R TR n - L TR n - L INT e - R INT n - L TR e - R TR n - R TR n - L INT e - R INT n - L TR n - L INT n - L TR e - L INT n - L TR e - R TR e - R TR n - L INT n - R INT n - R TR e - R INT n - R TR e - L INT e - L INT n - R TR e - R INT e - L INT n.

Phase 3: R TR n - R TR e - R INT n - R TR e - R INT e - R TR e - R INT n - R INT e - R INT n - R TR e - R INT n - R TR n - R TR n - R INT n - R TR n - R INT e - R TR e - R INT n - R TR e - R INT e - R TR n - R TR e - R TR e - R TR n - R INT e - R INT e - R INT n - R TR n - R TR n - R INT n - R INT e - R INT e.

References

H. Bekkering, A. Wohlschläger, and M. Gattis. Imitation of gestures in children is goal-directed. *Quarterly Journal of Experimental Psychology*, 2000.

E. Franz, S. Ford, and S. Werner. Brain and cognitive processes of imitation in bimanual situations: Making inferences about mirror neuron systems. *Brain Research*, 2007.

M. Iacoboni, R. Woods, M. Brass, H. Bekkering, J. Mazziotta, and G. Rizzolatti. Cortical mechanisms of human imitation. *Science*, 1999.

L. Koski, M. Iacoboni, M.-C. Dubeau, R. Woods, and J. Mazziotta. Modu-

	Average fixation time spent on each region (%):											
Subject	Center Region			Face			Right Arm			Left Arm		
Sub.1	36.61	35.28	45.00	5.55	3.10	6.56	24.31	15.65	18.71	0.35	16.10	0.00
Sub.2	97.87	94.45	98.38	0.00	0.00	0.00	0.00	0.00	0.00	0.00	0.14	0.00
Sub.3	24.47	11.81	3.36	59.29	53.34	39.89	2.30	1.22	15.63	0.00	2.63	0.50
Sub.4	59.21	20.70	21.40	23.47	5.62	13.99	0.46	1.90	6.85	0.78	4.02	2.17
Sub.5	41.03	34.40	51.74	27.62	17.83	17.49	13.78	8.05	8.82	0.00	14.49	0.00
Sub.6	19.75	13.32	3.75	68.86	56.06	57.09	1.16	8.14	29.01	0.00	12.25	0.00
Sub.7	77.12	62.34	70.68	12.21	8.19	13.43	0.00	3.31	2.00	0.00	9.56	0.00
Sub.8	47.35	36.62	52.55	25.20	22.42	34.36	0.00	0.10	0.49	1.04	5.26	0.47
Sub.9	55.32	43.00	4.71	8.00	6.70	9.31	6.65	15.44	28.79	0.00	14.29	1.70

Table A.1
Average percentage of viewing time spent fixating on each region for each subject and across the entire experiment.

lation of cortical activity during different imitative behaviors. *Journal of Neurophysiology*, 2003.

A. Meltzoff and M. Moore. Imitation, theory, and the representation of persons. *Infant Behavior & Development*, 2002.

A. Meltzoff and M. Moore. Imitation of facial and manual gestures by human neonates. *Science*, 1977.

A. Meltzoff and M. Moore. Explaining facial imitation: a theoretical model. *Early Development and Parenting*, 1997.

R. Oldfield. The assessment and analysis of handedness: the edinburgh inventory. *Neuropsychologia*, 1971.

G. Rizzolati, L. Fadiga, L. Fogassi, and V. Gallese. *The Imitative Mind: Development, Evolution and Brain Bases*, chapter From mirror neurons to imitation: facts and speculations. Cambridge University Press, 2002.

G. Rizzolatti, L. Fadiga, V. Gallese, and L. Fogassi. Premotor cortex and the recognition of motor actions. *Cognitive Brain Research*, 1996.

A. Wohlschläger, M. Gattis, and H. Bekkering. Action generation and action perception in imitation: an instance of the ideomotor principle. *Philosophical Transactions of the Royal Society*, 2003.